

**Linker Functionalization of a Bivalent Ligand for the Study of the
5-HT_{2A}R/ 5-HT_{2C}R Heterodimer**

A Thesis Presented to
the Faculty of the Department of Chemistry
University of Houston

In Partial Fulfillment
of the Requirements for the Degree
Master of Science

By
Lisa Thornsberry Yawn

August 2017

**Linker Functionalization of a Bivalent Ligand for the Study of the
5-HT_{2A}R/ 5-HT_{2C}R Heterodimer**

Lisa Thornsberry Yawn

Approved:

Dr. Scott R. Gilbertson, Chairman

Dr. Don M. Coltart

Dr. Olafs Daugulis

Dr. Arnold M. Guloy

Dr. Gregory D. Cuny

Dean, College of Natural Sciences
and Mathematics

Dedicated to
the glory of God,
to my husband, Kyle, for his constant support,
and to my parents, for laying the foundation for my education.

ACKNOWLEDGEMENTS

I would like to express my gratitude to the following people for their support throughout my graduate school experience.

To Dr. Scott Gilbertson, my research advisor.

To the members of my committee, Drs. Coltart, Cuny, Daugulis, and Guloy.

To all members of the Gilbertson group, both past and present.

Lisa Yawn

**Linker Functionalization of a Bivalent Ligand for the Study of the
5-HT_{2A}R/ 5-HT_{2C}R Heterodimer**

An Abstract of a Thesis Presented to
the Faculty of the Department of Chemistry
University of Houston

In Partial Fulfillment
of the Requirements for the Degree
Master of Science

By

Lisa Thornsberry Yawn

August 2017

ABSTRACT

G-protein-coupled receptors (GPCRs) are important pharmaceutical targets. In recent years, it has been found that GPCRs can function as homo- and hetero- dimers. The serotonin receptors 5-HT_{2A}R and 5-HT_{2C}R have been shown to form a heterodimer. These two receptors regulate impulsivity and cue reactivity, two factors that can lead to drug addiction relapse. A synergistic effect of the 5-HT_{2A}R antagonist M100907 and the 5-HT_{2C}R agonist WAY163909 in the suppression of impulsivity and cue reactivity has been reported. A bivalent ligand containing these two pharmacophores, linked by a polyethylene glycol chain and a triazole, has been developed.

In this thesis, attempts to functionalize the linker portion of the bivalent ligand for the addition of a fluorophore are reported. The first approach was to functionalize the triazole portion of the linker via the iodoalkyne-azide cycloaddition reaction; however, it was determined that this method was unsuitable due to challenges with purity and yield. The second approach was to functionalize the polyethylene glycol portion of the linker by replacing an oxygen atom with a nitrogen atom, allowing for tertiary substitution at the nitrogen. A linker was synthesized containing a tertiary amine in which an ester side-chain was included. This ester serves as a handle for incorporation of a fluorophore via amide coupling. A fluorophore-tagged bivalent ligand will open the door to cellular imaging of the 5-HT_{2A}R/5-HT_{2C}R GPCR heterodimer.

TABLE OF CONTENTS

Acknowledgements	iv
Abstract	vi
Table of Contents	vii
List of Abbreviations and Symbols	x
List of Figures	xiii
List of Schemes	xiv
Chapter I: Introduction to GPCR Dimers	1
1.1 Discovery and Physiological Relevance of GPCR Dimers	1
1.1.1 G-protein-coupled Receptors	1
1.1.2 GPCR Dimers	2
1.1.2.1 Discovery of GPCR Dimers	2
1.1.2.2 GPCR Heterodimers as Therapeutic Targets	2
1.1.2.3 Bivalent Ligands	4
1.2 Serotonin 2 _A and 2 _C Receptors	5
1.2.1 Relationship to Drug Relapse	5
1.2.2 Synergism Between 5-HT _{2A} R and 5-HT _{2C} R	6
1.2.3 Biological Evidence for 5-HT _{2A} R and 5-HT _{2C} R Dimerization	6
1.2.4 Bivalent Ligands for 5-HT _{2A} R and 5-HT _{2C} R	8
1.3 The Use of Fluorophores in Studying GPCR Dimers	9
1.3.1 Fluorescent Labelling of Monovalent Ligands and Receptors	9

1.3.2 Fluorophore-tagged Bivalent Ligands	11
Chapter II: Iodoalkyne Approach	14
2.1 Fluorophore-tagged Bivalent Ligand	14
2.2 Iodoalkyne-azide Cycloaddition Reaction	14
2.3 Results and Discussion	16
2.3.1 Model System	16
2.3.2 Alkyne Iodination	17
2.3.3 Cycloaddition	18
2.4 Conclusion	19
Chapter III: Tertiary Amine Approach	20
3.1 Overview of Synthetic Plan	20
3.2 Results and Discussion	21
3.2.1 Synthesis of Tertiary Amine	21
3.2.2 Synthesis of M100907 Derivative	22
3.2.3 Attachment of Functionalized Linker to M100907 Derivative	24
Chapter IV: Conclusion and Future Work	26
Chapter V: Experimental Section	32
5.1 General Methods	32

5.2 Experimental Procedures	33
5.3 NMR Spectra	40

LIST OF ABBREVIATIONS AND SYMBOLS

^1H NMR	^1H nuclear magnetic resonance spectrum
^{13}C NMR	proton decoupled ^{13}C nuclear magnetic resonance spectrum
5-HTR	5-hydroxytryptamine receptor (serotonin receptor)
δ	chemical shift in parts per million (NMR)
A _{2A} R	adrenergic receptor, type 2A
Boc	<i>tert</i> -butyloxycarbonyl
BRET	bioluminescence resonance energy transfer
<i>n</i> -BuLi	<i>n</i> -butyl lithium
CCK ₂ R	cholecystokinin receptor, type 2
CuAAC	copper-catalyzed azide-alkyne cycloaddition
CXCR4	chemokine receptor, type 4
Cy5	cyanine 5
d	doublet (NMR)
D ₂ R	dopaminergic receptor, type 2
DCM	dichloromethane
dd	doublet of doublets (NMR)
DIPEA	N,N-diisopropylethylamine
DMAP	4-(dimethylamino)pyridine
DMF	dimethylformamide
Et	ethyl

Eu-DTPA	europium-diethylenetriaminepentaacetic acid
FCS	fluorescence correlation spectroscopy
FDA	Food and Drug Administration
FPR	formyl peptide receptor
FRET	fluorescence resonance energy transfer
g	gram
GABA	gamma-aminobutyric acid
GLP-1R	glucagon-like peptide-1 receptor
GPCR	G-protein-coupled receptor
GTP	guanosine triphosphate
HBTU	(2-(1H-benzotriazol-1-yl)-1,1,3,3-tetramethyluronium hexafluorophosphate)
HMQC	heteronuclear multiple quantum coherence
HOAc	acetic acid
Hz	Hertz
IBX	2-iodoxybenzoic acid
<i>J</i>	scalar coupling constant (NMR)
KHMDS	potassium hexamethyldisilane
LC-MS	liquid chromatography-mass spectrometry
m	multiplet (NMR)
M ₁ R	muscarinic acetylcholine receptor, type 1
Me	methyl
mg	milligram

mL	milliliter
mmol	millimole
NMR	nuclear magnetic resonance
PEG	polyethylene glycol
ppm	parts per million
RT	room temperature
s	singlet (NMR)
STAB	sodium triacetoxyborohydride
SUR1	sufonylurea-1 receptor
t	triplet (NMR)
TBAF	tetrabutylammonium fluoride
TBDPS	<i>tert</i> -butyldiphenylsilyl
TEMPO	(2, 2, 6, 6-tetramethylpiperidin-1-yl)oxy
TFA	trifluoroacetic acid
THF	tetrahydrofuran
TMEDA	tetramethylethylenediamine
Ts	tosyl

LIST OF FIGURES

Figure 1.1. Structure of a GPCR.	1
Figure 1.2. Heterobivalent ligand.	4
Figure 1.3. The entropic advantage of bivalent ligands.	5
Figure 1.4. 5-HT _{2A} R antagonist, 5-HT _{2C} R agonist, and bivalent ligands.	9
Figure 1.5. Different methods of incorporating a fluorophore into a bivalent ligand.	12
Figure 2.1. Addition of a fluorophore to the triazole of the linker.	15
Figure 2.2. Iodoalkyne and azide selected as model system for cycloaddition.	16
Figure 3.1. Tertiary amine strategy.	20

LIST OF SCHEMES

Scheme 2.1. Synthetic plan for adding a fluorophore to the triazole of the linker.	15
Scheme 2.2. Synthesis of azide and terminal alkyne.	17
Scheme 2.3. Iodination of terminal alkyne.	17
Scheme 2.4. Cycloaddition of crude alkyne mixture with azide 2.2 .	18
Scheme 2.5. Cycloaddition with commercially available 1-iodoalkyne.	19
Scheme 3.1. Synthesis of tertiary amine linker.	21
Scheme 3.2. Reductive amination under acidic conditions yielded a dialkylated amine.	22
Scheme 3.3. Synthesis of a derivative of 5-HT _{2A} R antagonist M100907.	23
Scheme 3.4. Synthesis of compounds 3.7 and 3.12 .	24
Scheme 3.5. Tosylation of tertiary amine.	24
Scheme 3.6. Attachment of tosylated linker to 3.14 was attempted with NaH and KHMDS as the base.	25

Chapter I: Introduction to GPCR Dimers

1.1 Discovery and Physiological Relevance of GPCR Dimers

1.1.1 G-protein-coupled Receptors

G-protein-coupled receptors (GPCRs) are proteins which span the cell membrane and transmit signals from the outside of the cell to the inside of the cell via activation of a G-protein, that is, a protein which binds guanosine triphosphate (GTP). The G-protein in turn activates a cascade of intracellular signaling. The roles of different GPCRs vary greatly; agonists for GPCRs include neurotransmitters, hormones, and even light. While there is a great diversity of structure and function within the GPCR superfamily, nearly all GPCRs are characterized by seven transmembrane α -helices, an extracellular N-terminus, and an intracellular C-terminus (Figure 1.1). GPCRs are an important pharmacological target, with approximately one-third of small-molecule drugs approved by the Food and Drug Administration (FDA) targeting GPCRs.¹

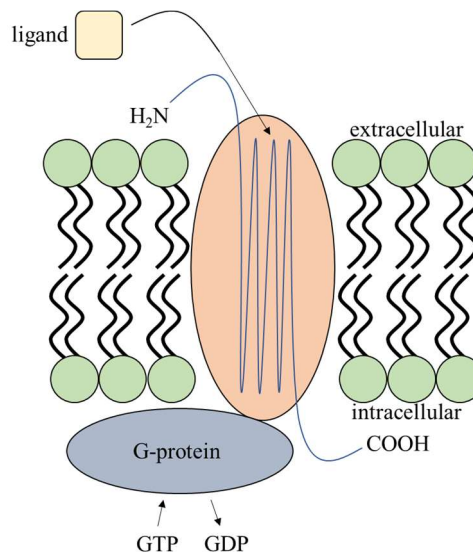


Figure 1.1. Structure of a GPCR. When the ligand binds, the signal is transmitted from the outside to the inside of the cell via activation of the G-protein.

1.1.2 GPCR Dimers

1.1.2.1 Discovery of GPCR Dimers

Since the characterization of GPCRs in the 1970s-80s^{2,3} until the late 1990s, GPCRs were widely believed to exist as monomers. Due to the membrane solubilization technique required to isolate GPCRs from the lipid bilayer and characterize them in aqueous solution, GPCR dimers and oligomers were not observed, and GPCRs were assumed to function in a monomeric fashion. In 1998, studies^{4,5} of the gamma-aminobutyric acid (GABA) receptors GABA_BR1 and GABA_BR2 in living, recombinant cells revealed that when GABA_BR2 is not expressed, GABA_BR1 is not transported from the endoplasmic reticulum to the cell membrane; furthermore, coimmunoprecipitation indicated that the two receptors are colocalized on the cell membrane. The discovery that these two GABA receptors functioned as a heterodimer (that is, two different GPCRs forming one functional unit) marked a paradigm shift in the understanding of GPCRs.

In subsequent years, recombinant cell lines were used to show the existence of many more GPCR heterodimers as well as homodimers (that is, two of the same GPCRs forming one functional unit). However, in recombinant cell lines, receptors are often expressed at levels much higher than they would be *in vivo*, and some of the early data has been called into question.⁶ Controversy persists as to whether GPCRs form higher-order oligomers, whether GPCR dimers exist in equilibrium with monomers, and whether some reported GPCR dimers are functionally relevant.

1.1.2.2 GPCR Heterodimers as Therapeutic Targets

A major motivation in studying GPCR heterodimers is that they may prove to be valuable targets for novel therapeutics. GPCR heterodimers can exhibit different

properties than monomers or homodimers, and so modulating the activity of heterodimers potentially offers a new strategy in drug design. Additionally, a drug designed to target a heterodimer may lead to greater potency, better specificity, and fewer off-target effects.

In some cases, one protomer of a heterodimer can allosterically modulate the affinity of the other protomer for a ligand. In the A_{2A} adrenergic receptor- D₂ dopaminergic receptor heterodimer,⁷ for example, antagonism of A_{2A}R increases the affinity of D₂R for dopamine.⁸ Primate trials have shown that administration of an A_{2A} antagonist can be used to increase affinity for constitutive dopamine, and co-administration of an A_{2A} antagonist with L-dopa (a precursor to dopamine) can be used to decrease the extent of dyskinesia that is often a side effect of L-dopa.⁹

Another approach to novel therapeutics is by either inducing or interrupting the formation of GPCR heterodimers. For example, the μ -opioid receptor (MOR) and type 2 cholecystinin receptor (CCK₂R) do not form constitutive heterodimers, but when treated with a compound bearing pharmacophores for both receptors, heterodimer formation is induced.¹⁰ CCK₂R modulates opioid tolerance, and in proof-of-principle *in vivo* studies, this strategy was shown to reduce morphine tolerance in mice. On the other hand, blocking the formation of constitutive dimers can also yield a therapeutic advantage, though this approach has been more frequently tested in homodimers rather than heterodimers. In a 2005 study,¹¹ the disruption of the formyl peptide receptor (FPR) of neutrophils with a peptide that inhibits the association of the transmembrane domains of the protomers resulted in increased superoxide production.

1.1.2.3 Bivalent Ligands

A major contribution to the study of GPCR dimers from the field of chemistry has been the development of bivalent ligands. In these compounds, two ligands are joined together by a tether, also known as a linker (Figure 1.2). Bivalent ligands may either be homobivalent, in which both pharmacophores are the same, or heterobivalent, in which each pharmacophore is selective for a different receptor.

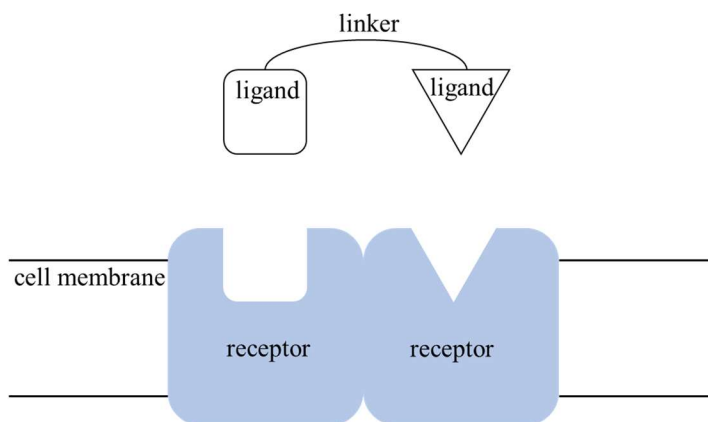


Figure 1.2. Heterobivalent ligand. Two ligands, each selective for a one of the receptors of the dimer, are joined by a linker.

Such compounds were first developed by Portoghese¹² in 1982 to estimate the distance between opioid receptor subtypes by testing different linker lengths. The increased potency of the bivalent ligands in this study was attributed to the entropic advantage of binding the second pharmacophore of the singly-bound bivalent ligand when compared the entropy cost of binding a free bivalent ligand (Figure 1.3).¹³ The applicability to the study of GPCR dimers was only recognized later.

The design of a bivalent ligand depends first upon the availability of ligands that are selective for each of the receptors in question. Each ligand must have a location to

which the tether may be attached without adversely affecting the binding and efficacy of the compound. To test this requirement, the ligand can be synthesized with the linker or a proxy for the linker in place, but without the second pharmacophore. Another important consideration in the design of the bivalent ligand is the type of linker. Though this can be a simple hydrocarbon chain, more commonly polyethylene glycol or polyamide chains are used so that the molecule does not become too hydrophobic, which would pose a risk of entrapment in the lipophilic interior of the cell membrane.

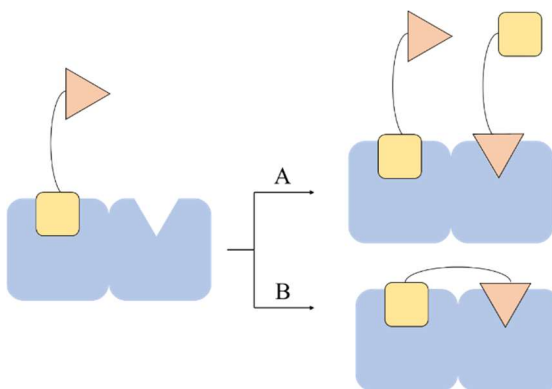


Figure 1.3. The entropic advantage of bivalent ligands. In pathway (A), a second heterobivalent ligand binds to the second receptor. In pathway (B), the second pharmacophore of the first heterobivalent ligand binds to the second receptor. Pathway (B) represents a lower entropic cost.

1.2 Serotonin 2_A and 2_C Receptors

1.2.1 Relationship to Drug Relapse

A putative GPCR heterodimer that is of interest to our group is that of the serotonin (5-HT) 2_A receptor (5-HT_{2A}R) and serotonin 2_C receptor (5-HT_{2C}R) due to the relationship between these receptors and drug abuse relapse. The return to taking drugs after an extended period of abstinence is a major problem in addiction treatment, with 40-

60% of recovering addicts experiencing at least one relapse during their recovery.¹⁴ Relapse has been linked to impulsivity, defined as the tendency to act without considering negative consequences,¹⁵ and cue reactivity, defined as the tendency to respond to cues associated with drug-taking.¹⁶ These two factors are reduced by antagonism of the 5-HT_{2A}R.^{17,18} The 5-HT_{2C}R works in opposition¹⁹ to the 5-HT_{2A}R; that is, agonism of the 5-HT_{2C}R reduces impulsivity²⁰ and cue-reactivity.²¹

1.2.2 Synergism Between 5-HT_{2A}R and 5-HT_{2C}R

An early indication that the 5-HT_{2A}R and 5-HT_{2C}R may form heterodimers was reported by our collaborators in a rat behavioral study.²² By co-administering a subthreshold dose of a 5-HT_{2A}R antagonist (M100907) with a subthreshold dose of a 5-HT_{2C}R agonist (WAY163909), either of which would be ineffective on its own, significant changes to the rats' behavior were observed. Specifically, rats who were treated with the two compounds together showed a decrease in cocaine-induced motor activity (though not spontaneous motor activity), a decrease in both inherent and cocaine-induced impulsive action, and a decrease in both cue-induced and cocaine-primed reinstatement of cocaine self-administration (relapse). The ability of subthreshold doses of the two compounds to elicit a response suggests that the 5-HT_{2A}R and 5-HT_{2C}R act synergistically rather than independently of one another, and although no mechanism of this synergism was observable in these animal studies, a plausible explanation would be that the 5-HT_{2A}R and 5-HT_{2C}R form a heterodimer.

1.2.3 Biological Evidence for 5-HT_{2A}R and 5-HT_{2C}R Dimerization

Recent biological data provide strong evidence for the existence of 5-HT_{2A}R and 5-HT_{2C}R homodimers and heterodimers.²³ In cells transfected with 5-HT_{2A}R that had been

linked to fluorescent proteins, bioluminescence resonance energy transfer (BRET, discussed below) was used to show that these receptors are in close proximity to one another, most likely indicating homodimerization. The same result was observed for cells expressing fluorescent 5-HT_{2C}R. In cells expressing both 5-HT_{2A}R and 5-HT_{2C}R, not only was the BRET response indicative of heterodimer formation but also that heterodimerization is preferred over homodimerization. Co-immunoprecipitation was used to confirm the physical interaction of 5-HT_{2A}R and 5-HT_{2C}R.

In signaling studies of the 5-HT_{2A}R/5-HT_{2C}R dimer, the 5-HT_{2C}R was found to be dominant over the 5-HT_{2A}R. When cells were first treated with a 5-HT_{2A}R antagonist and then with 5-HT, no significant difference in signaling was detected as measured by the amount of downstream inositol phosphate produced; thus, deactivation of the 5-HT_{2A}R had no effect on signaling. However, when the cells were treated with a 5-HT_{2C}R antagonist and then with 5-HT, signaling was significantly decreased; thus, 5-HT_{2C}R is the main contributor to signaling. Similar results were observed in mouse neurons and in live mice.

The recent finding that the 5-HT_{2C}R is dominant over the 5-HT_{2A}R is consistent with the previous observation that subthreshold doses of a 5-HT_{2C}R agonist and 5-HT_{2A}R antagonist significantly affect the impulsivity and cue reactivity of rats. Though much further study is needed, one possible explanation is that some monomeric or homodimeric 5-HT_{2A}Rs are blocked by the antagonist while others are blocked by heterodimerization with 5-HT_{2C}R, leading to more deactivation of the 5-HT_{2A}R than would be expected from a monomeric model of these GPCRs.

1.2.4 Bivalent Ligands for 5-HT_{2A}R and 5-HT_{2C}R

To study the properties of 5-HT_{2A}R and 5-HT_{2C}R homodimers and probe the existence of heterodimers, bivalent ligands have been synthesized by our group (Figure 1.4). A homobivalent ligand of the 5-HT_{2A}R antagonist M100907 was synthesized with a polyethylene glycol (PEG) linker of varying lengths.²⁴ When tested in cells expressing the 5-HT_{2A}R, the bivalent ligands with linkers ranging from 12 to 18 atoms were found to be the most potent; this specificity of length is strong evidence for homodimerization because it indicates that the bivalent linker is the appropriate length to span the distance between the two receptors. The 5-HT_{2A}R was later shown to form homodimers via biological methods.^{25, 26}

A heterobivalent ligand was synthesized from M100907 and WAY163909, a 5-HT_{2C}R agonist, to target the presumed 5-HT_{2A}R and 5-HT_{2C}R heterodimer.^{27,28} To accomplish this, a PEG linker bearing an azide group was attached to M100907, and a PEG linker bearing an alkyne group was attached to WAY163909. The two pharmacophores were linked via the copper-catalyzed azide-alkyne cycloaddition (CuACC). Ligands with various tether lengths were synthesized, and the one with the 17-atom linker had the most promising biological activity in cells expressing both 5-HT_{2A}R and 5-HT_{2C}R, though further testing is needed to confirm this result.

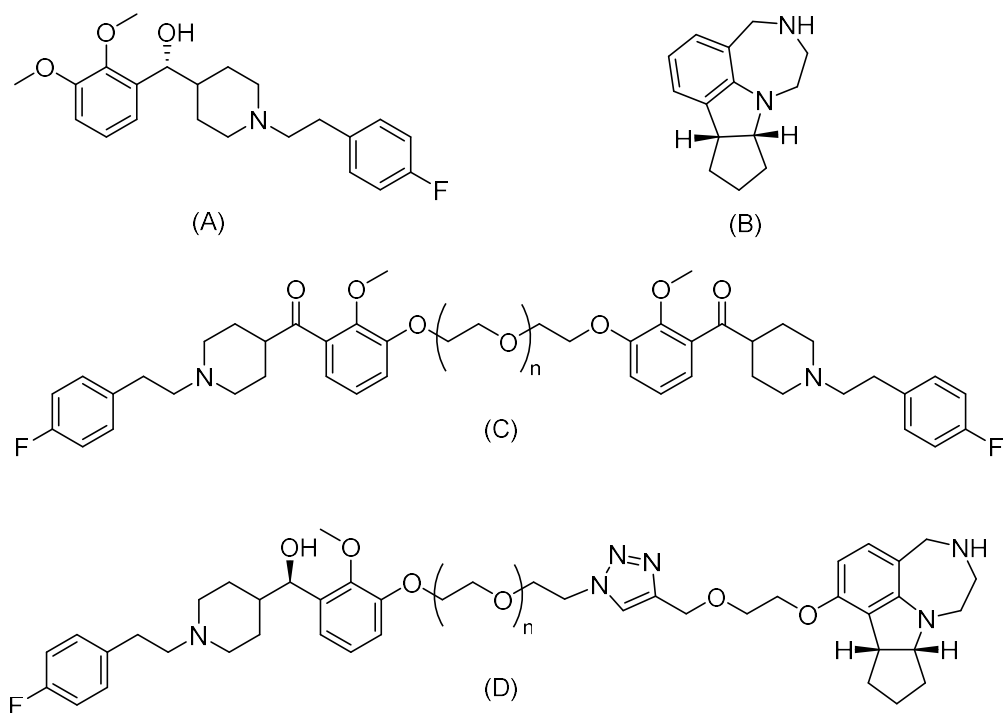


Figure 1.4. 5-HT_{2A}R antagonist, 5-HT_{2C}R agonist, and bivalent ligands. (A) M100907, a 5-HT_{2A}R antagonist. (B) WAY163909, a 5-HT_{2C}R agonist. (C) Homobivalent M100907. The stereogenic hydroxyl group was replaced with a ketone as a synthetic simplification. (D) Heterobivalent M100907-WAY163909.

1.3 The Use of Fluorophores in Studying GPCR Dimers

1.3.1 Fluorescent Labelling of Monovalent Ligands and Receptors

The use of fluorescence imaging, both with small-molecule organic fluorophores as well as with fluorescent proteins, has been crucial in developing an understanding of the existence of GPCR dimers and oligomers, their lifetime, and their size. Resonance energy transfer techniques (BRET and fluorescence resonance energy transfer, FRET) have been invaluable in the study of GPCR dimers. BRET and FRET occur via the transfer of energy from a donor fluorophore to an acceptor fluorophore which can only occur at distances of approximately 1-10 nanometers²⁹ and decreases sharply at greater

distances. Thus, if the acceptor fluorophore exhibits fluorescence, then the donor and acceptor are close to one another. This technique has been used to support the existence of many GPCR dimers, both by fluorescently labeling ligands and by fluorescently labeling the receptors themselves as with the 5-HT_{2A}R/5-HT_{2C}R heterodimer discussed above.²³ A limitation of BRET and FRET is that it is possible for a donor and acceptor to be close enough to give a fluorescent signal without the two receptors being in physical contact; these methods can give strong support for the existence of a dimer or oligomer, but they are not conclusive.³⁰

Another technique used is fluorescence correlation spectroscopy (FCS), in which either fluorescence-tagged receptors or receptors bound to fluorescence-tagged ligands move in and out of an observation area, and the changes in fluorescence are detected over time. Based on the premise that GPCR dimers move through the cell membrane more slowly than monomers, FCS was used to show that the 5-HT_{2C}R forms homodimers and not monomers when singly expressed.³¹

The introduction of super-resolution nanoscopy has opened the door to single-molecule tracking using fluorophores. In a landmark study³² in 2010, Hern *et al.* administered a monovalent fluorescent ligand to live cells expressing the M₁ muscarinic acetylcholine receptor and followed the movement of the receptors via video. By analyzing the intensity of fluorescence, both the formation and dissociation of homodimers was observed. This finding introduced the idea that GPCR monomers and dimers exist in a dynamic equilibrium. For the M₁ receptor, approximately 30% of receptors existed as dimers at a given time, and the lifetime was about 0.5 seconds. The Kasai group reported similar findings for the N-formyl peptide receptor, in that the

lifetime was about 150 milliseconds.³³ In these studies and others, fluorescence-labeled ligands have been valuable tools to further understand the nature of GPCR dimers.

1.3.2 Fluorophore-tagged Bivalent Ligands

While bivalent ligands have been a valuable tool for selectively targeting GPCR dimers, and fluorescence-labelled monovalent ligands have been key in imaging GPCR dimers via the techniques recounted above, relatively few bivalent ligands have incorporated a fluorophore to allow for visualization of the dimeric receptor. In a 2010 study, a homobivalent ligand for the chemokine receptor CXCR4 was tagged with the fluorophore tetramethylrhodamine.³⁴ The linker was composed of a rigid poly-L-proline segment as a means of estimating the distance between the two receptors. A lysine residue was incorporated into the linker so that the amine side-chain could be used as a handle for the second pharmacophore. The fluorophore was attached to the amino acid chain by means of an amide bond. A similar approach was used in the development of a heterobivalent ligand for the melanocortin and cholecystokinin receptors.³⁵ The linker composed of flexible PEG segments and a semiflexible alternating proline-glycine segment, and incorporation of a lysine residue at the junction of these two segments provided a handle on which to attach a fluorophore (Figure 1.5 A). Cyanine (Cy5) or europium (Eu-DTPA) was incorporated into the linker in this way. This strategy was repeated by the same group in the development of a heterobivalent ligand for the sulfonylurea-1 receptor (SUR1) and glucagon-like peptide-1 receptor (GLP-1R), except rather than using a lysine side-chain as a fluorophore handle, a cysteine residue was used.³⁶ The Cy5 was modified to contain a maleimide to form a bond to the sulfur atom of the cysteine (Figure 1.5 B). Another method of incorporating a fluorophore into a

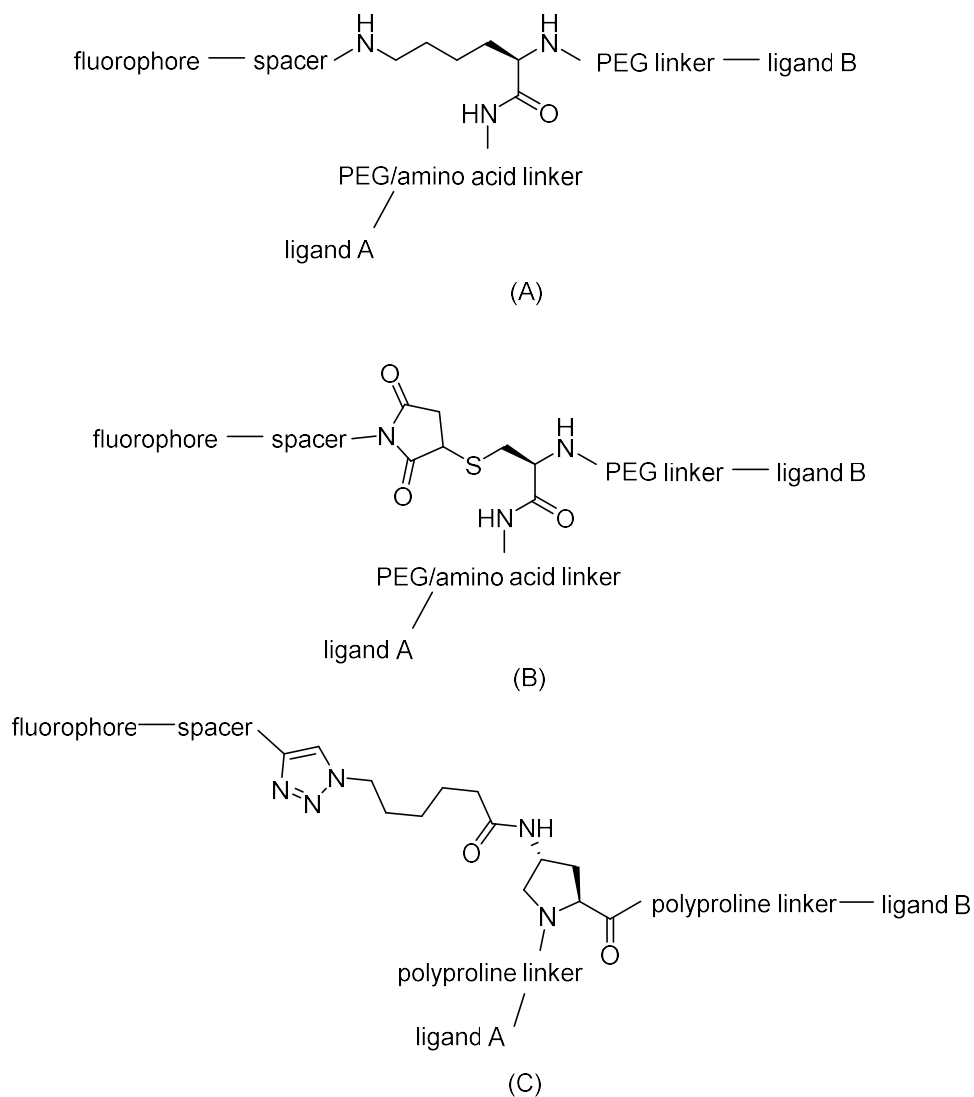


Figure 1.5. Different methods of incorporating a fluorophore into a bivalent ligand. (A) The fluorophore is attached via the side chain of a lysine residue. (B) The fluorophore is attached via the side chain of a cysteine residue. (C) The fluorophore is attached via a modified proline residue and the copper-catalyzed azide-alkyne cycloaddition.

poly-L-proline linker was developed by modifying one of the proline residues before adding it to the linker so that it contained an azide, and the fluorophore was then added through the copper-catalyzed azide-alkyne cycloaddition (Figure 1.5 C).³⁷ The use of an amino acid as a means of incorporating a fluorophore is convenient when the linker is

itself composed of amino acids, especially as this strategy is compatible with solid-phase synthesis techniques. However, no examples exist of a fluorophore incorporated into a PEG-only linker.

The incorporation of fluorophores into the bivalent ligands described above allowed for valuable biological information to be acquired. Cells with high expression of CXCR4 were distinguished from cells with medium and low expression of this receptor by use of the fluorescent homobivalent ligand; the monovalent ligand did not show a large enough difference in binding affinity to effectively distinguish among these cell types. As overexpression of CXCR4 has been implicated in cancer metastasis, the homobivalent ligand has been proposed as a cancer diagnostic. The fluorescent heterobivalent ligand for MC1R-CCK2R was tested *in vivo* in tumors grafted into the flanks of mice. The bivalent ligand selectively targeted the tumors expressing both receptors over tumors expressing only one receptor (as detected by fluorescence measurements), demonstrating a proof-of-principle that bivalent ligands can be used to enhance specificity of binding to particular cells or tissues. The fluorescent heterobivalent ligand for SUR1 and GLP-1R yielded similar results in pancreatic β -cells, though the binding was only specific at low concentrations of ligand. Additionally, in both of these heterobivalent studies, the fluorophore allowed for the visualization of ligand binding and subsequent internalization of the receptor into the cell.

Chapter II: Iodoalkyne Approach

2.1 Fluorophore-tagged Bivalent Ligand

In order to visualize the 5-HT_{2A}R/5-HT_{2C}R heterodimer on living cells, the objective of adding a fluorophore to the bivalent M100907-WAY163909 ligand was determined. As in the studies mentioned above,³⁵⁻³⁷ adding a fluorophore can also allow for the assessment of selectivity of the heterobivalent ligand for the heterodimer and determination of whether the ligand is internalized after binding. One important aspect that was considered in the design of the fluorophore-tagged ligand was keeping the compound as similar as possible to previously synthesized bivalent M100907-WAY163909 ligands to minimize variability introduced into biological testing. Another aspect was to provide a site for the addition of a fluorophore that would be complementary with the functional groups available on commercially available fluorophores. Additionally, the fluorophore could not be too close to either ligand so that it would not interfere with receptor binding.

2.2 Iodoalkyne-azide Cycloaddition Reaction

The first approach to add a handle for a fluorophore to the bivalent M100907-WAY163909 ligand that would satisfy these requirements was to functionalize the triazole of the linker (Figure 2.1). This strategy employed the use of the copper-catalyzed cycloaddition of an azide with a 1-iodoalkyne developed by Sharpless, Fokin, and coworkers.³⁸ Like the copper-catalyzed azide-alkyne cycloaddition previously used by members of our group to synthesize the M100907-WAY163909 bivalent ligand, the iodo-

variation makes use of orthogonal functional groups on each side of the bivalent linker, which would enable the linkage of the two ligands late in the synthesis with little or no interference with the functional groups present on either ligand.

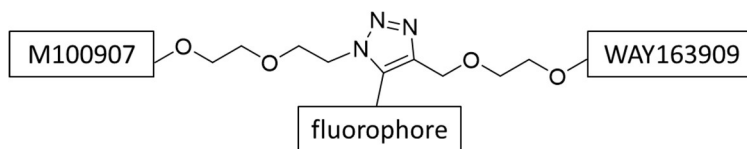
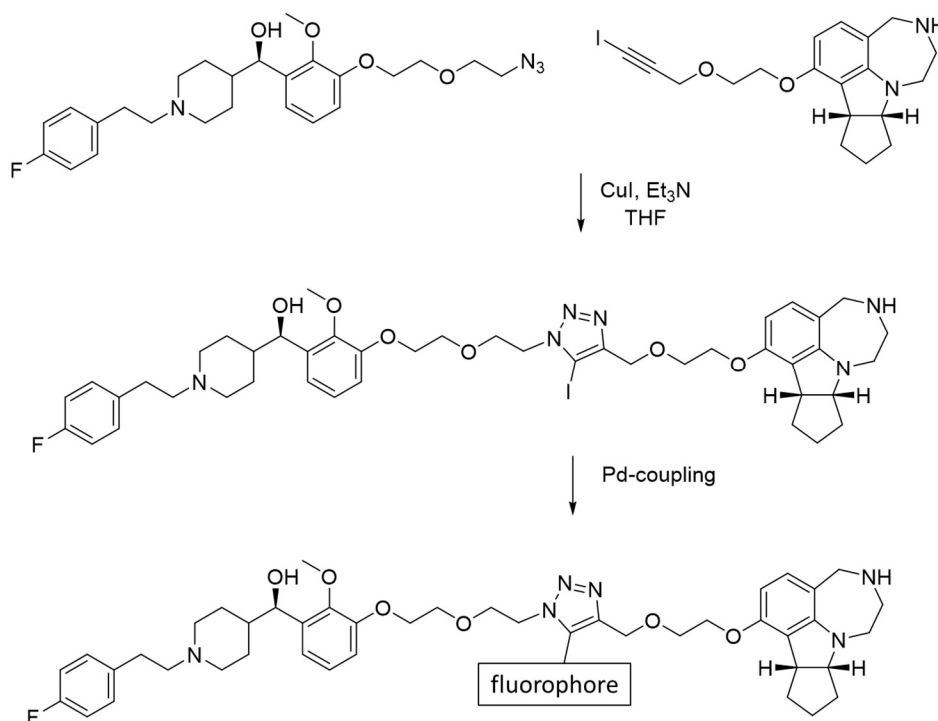


Figure 2.1. Addition of a fluorophore to the triazole of the linker.

The advantage of using a 1-iodoalkyne rather than a terminal alkyne is that the 5-iodotriazole formed in the cycloaddition can be used in cross-coupling reactions, and a fluorophore containing the appropriate reactive functional group could then be added at the 5-position of the triazole via Suzuki, Heck, or Sonogashira coupling.



Scheme 2.1. Synthetic plan for adding a fluorophore to the triazole of the linker.

Though the cycloaddition is completely regioselective for the 5-iodotriazole over the 4-iodotriazole, the type of ligand used can greatly affect the yield of the reaction and the amount of prototriazole that is also formed.

2.3 Results and Discussion

2.3.1 Model System

The cycloaddition of an azide and a 1-iodoalkyne was first attempted on a model system consisting of the linker portion of the bivalent ligand without the ligands themselves. The molecules to be used in the model system are shown in Figure 2.2.

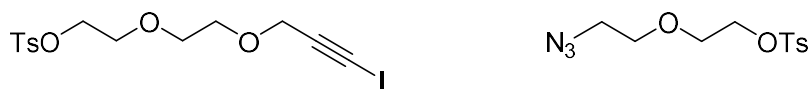
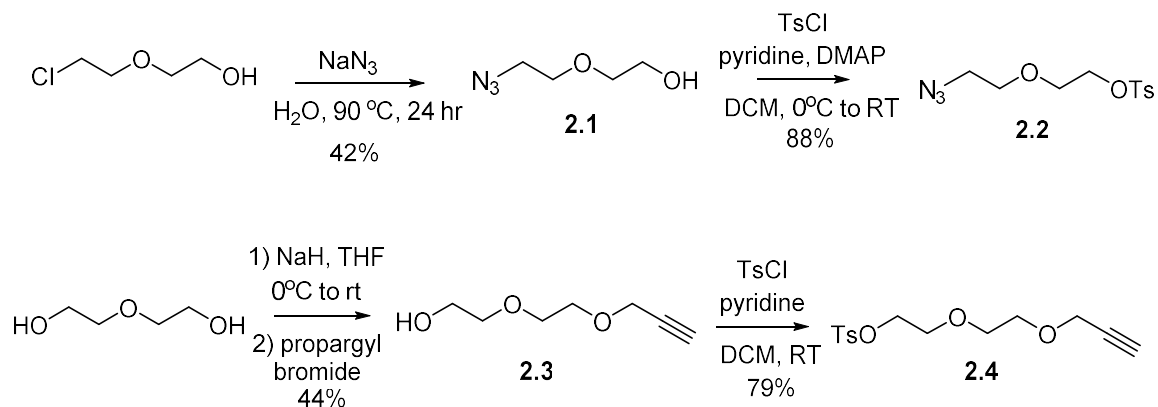


Figure 2.2. Iodoalkyne and azide selected as model system for cycloaddition.

The azide had previously been synthesized in our group, as well as the alkyne that did not contain iodine (Scheme 2.2). The use of the tosyl group greatly increased the ultraviolet absorption of the compounds, making the reactions easier to follow by thin-layer chromatography, and when needed this group could be used as a leaving group.

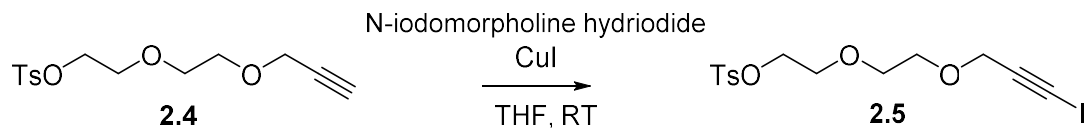
The azide (**2.2**) was synthesized in two steps from starting material 2-(2-chloroethoxy)ethanol. First, the chloride was displaced by the azide via substitution, and then the hydroxyl group was tosylated. The terminal alkyne (**2.4**) was synthesized in similar fashion from diethylene glycol. First, the propargyl group was added, and then the hydroxyl group was tosylated.



Scheme 2.2. Synthesis of azide and terminal alkyne.

2.3.2 Alkyne Iodination

The terminal alkyne **2.4** was iodinated using N-iodomorpholine hydriodide (Scheme 2.3) according to the method reported by Sharpless, Fokin, and coworkers.³⁸



Scheme 2.3. Iodination of terminal alkyne.

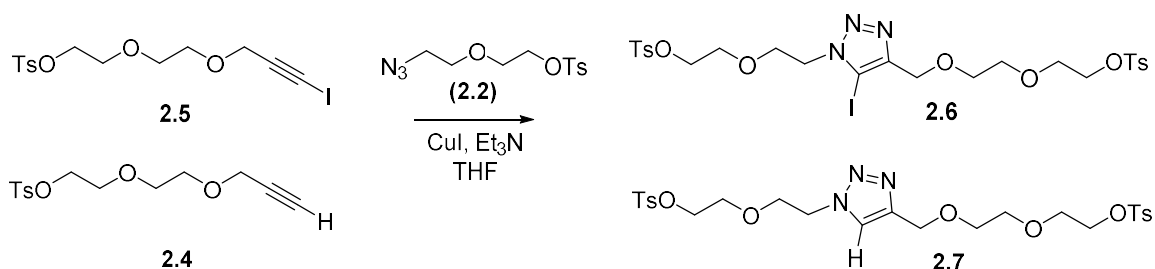
In the reported procedure for other iodoalkynes synthesis by this method, the compounds were filtered through activated, neutral alumina and used in the cycloaddition reaction without further purification. Isolation of compound **2.5** was attempted using silica gel chromatography; however, the nearly identical retention factors of the product and starting material prevented a clean separation.

Though the product was not cleanly isolated, the crude ¹H NMR spectrum shows the disappearance of the proton of the terminal alkyne. The methylene group adjacent to the alkyne shifts downfield and is no longer coupled to the acetylene proton. Also, low-

resolution liquid chromatography- mass spectrometry (LC-MS) shows the expected mass to charge ratio of 425 for the iodoalkyne, as well as the mass to charge ratio of 299 for the protoalkyne. These data indicate that the iodination reaction was indeed successful.

2.3.3 Cycloaddition

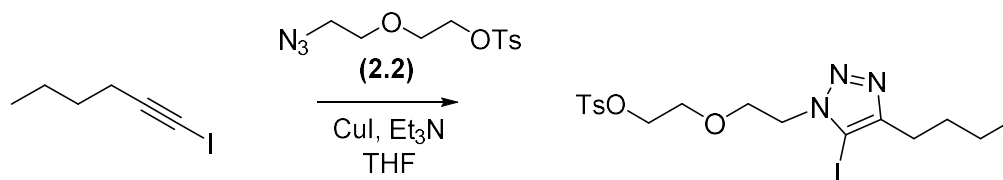
Though the iodoalkyne could not be cleanly isolated, the cycloaddition reaction with the azide was attempted with the crude product of the iodination reaction following the one-pot, two-step protocol reported by Sharpless, Fokin, and coworkers (Scheme 2.4).³⁸ The crude alkyne product was filtered through celite into a pre-mixed solution of copper iodide and triethylamine in tetrahydrofuran. The result, as determined by LC-MS, was a complex mixture of the azide starting material, both the proto- and iodo- alkynes, and both the proto- and iodo- triazole. The desired product could not be separated from this complex mixture.



Scheme 2.4. Cycloaddition of crude alkyne mixture with azide 2.2.

It has been reported that the type and amount of amine ligand can determine the ratio of prototriazole to iodotriazole; however, since the alkyne mixture could not be separated, it could not be determined the extent to which iodine was lost during the reaction. The cycloaddition was thus attempted with commercially available 1-

iodohexyne to ensure the purity of the iodoalkyne (purity was verified by ^1H NMR before use). Only the iodotriazole was formed, indicating that for this model system, iodine was not lost during the cycloaddition.



Scheme 2.5. Cycloaddition with commercially available 1-iodoalkyne.

2.4 Conclusion

Given the challenges in purification and yield that were encountered in the model system, it was determined that the azide-iodoalkyne cycloaddition reaction would not be a suitable method to functionalize the linker of the bivalent M100907-WAY163909 ligand. Because the iodinated linker could not be purified, addition of the linker to either M100907 or WAY163909 would result in some of the protoalkyne linker being added, lowering yield of the desired product late in the synthesis. Though functionalizing the triazole of the linker would lead to a bivalent ligand most similar to those previously synthesized by our group and tested on cells, the mixed results of the iodination reaction compromised the practicality of this approach.

Chapter III: Tertiary Amine Approach

3.1 Overview of synthetic plan

As an alternative to the iodoalkyne-azide cycloaddition reaction, a strategy was developed using a tertiary amine to incorporate a handle for a fluorophore. In this approach, one of the oxygen atoms of the PEG linker is replaced with a nitrogen (Figure 3.1). This nitrogen atom enables tertiary substitution without the addition of a stereocenter, as would be the case with a tertiary carbon. Additionally, the change from oxygen to nitrogen does not significantly change the polar surface area of the compound, which is necessary to consider as these compounds will be used for biological testing.

A methyl ester was chosen as the fluorophore handle to install on the linker. Many commercially available fluorophores contain an amine functional group, so the fluorophore could then be attached to the linker by an amide coupling. In fact, fluorophores containing an amine are more common commercially than fluorophores containing a boronic acid needed for Suzuki coupling, making this approach more versatile than the iodoalkyne approach described in Chapter 2.

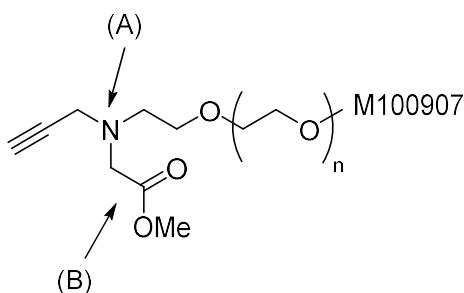
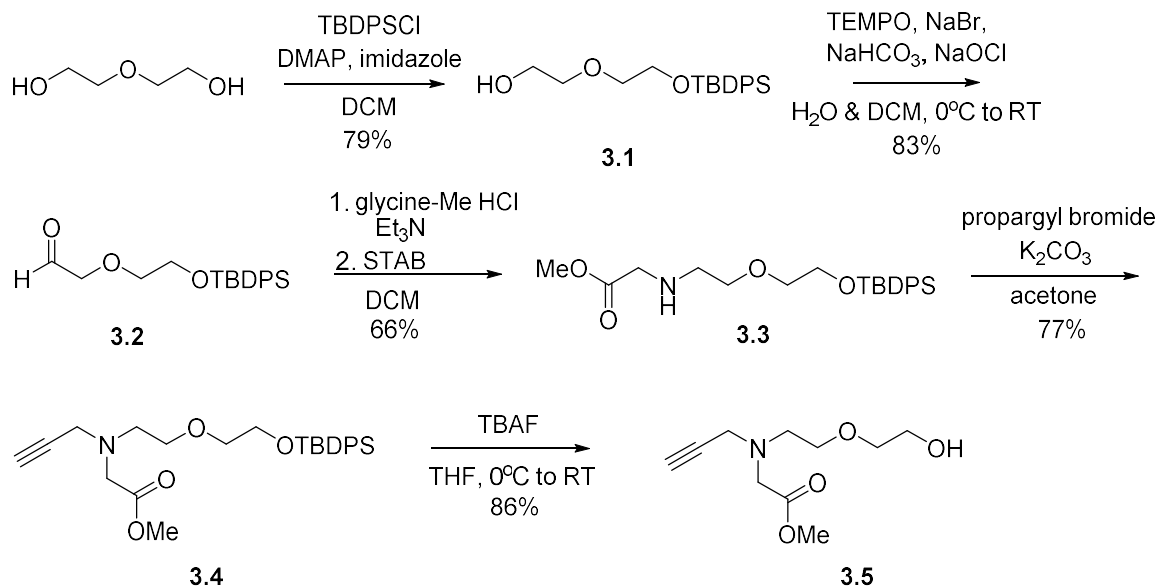


Figure 3.1. Tertiary amine strategy. (A) An oxygen atom in the PEG linker is substituted for a nitrogen to allow tertiary substitution. (B) A methyl ester is used as a handle for attachment of a fluorophore via amide coupling.

3.2 Results and Discussion

3.2.1 Synthesis of Tertiary Amine

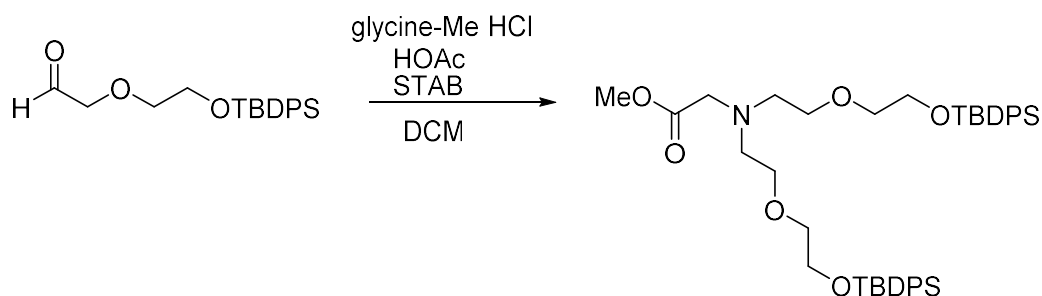
The linker with the tertiary amine was synthesized from diethylene glycol according to Scheme 3.1. One hydroxyl group of diethylene glycol was protected as a silyl ether (**3.1**). The other hydroxyl group was then oxidized to the aldehyde (**3.2**). Several oxidation methods were tested, including the use of 2-iodoxybenzoic acid (IBX) and the Swern oxidation. All methods gave comparable yields, and the use of bleach and (2, 2, 6, 6-tetramethylpiperidin-1-yl)oxy (TEMPO) was favored due to the short reaction time of two hours.



Scheme 3.1. Synthesis of tertiary amine linker.

The amine group, as well as the ester for later amide coupling, were added via reductive amination with glycine methyl ester hydrochloride. The amination was first attempted under acidic conditions because such conditions have been reported to increase

the rate of reaction by protonating the aldehyde, which accelerates the formation of the imine.³⁹ However, under acidic conditions, only a trace amount of the dialkylated amine was isolated (Scheme 3.2) and the desired monoalkylated amine was not formed. The conditions were then altered so that the glycine methyl ester hydrochloride salt was first mixed with one equivalent of triethylamine. The neutralized amine was then added to aldehyde **3.2** along with sodium triacetoxyborohydride (STAB), which gave the desired secondary amine (**3.3**) in good yield.



Scheme 3.2. Reductive amination under acidic conditions yielded a dialkylated amine.

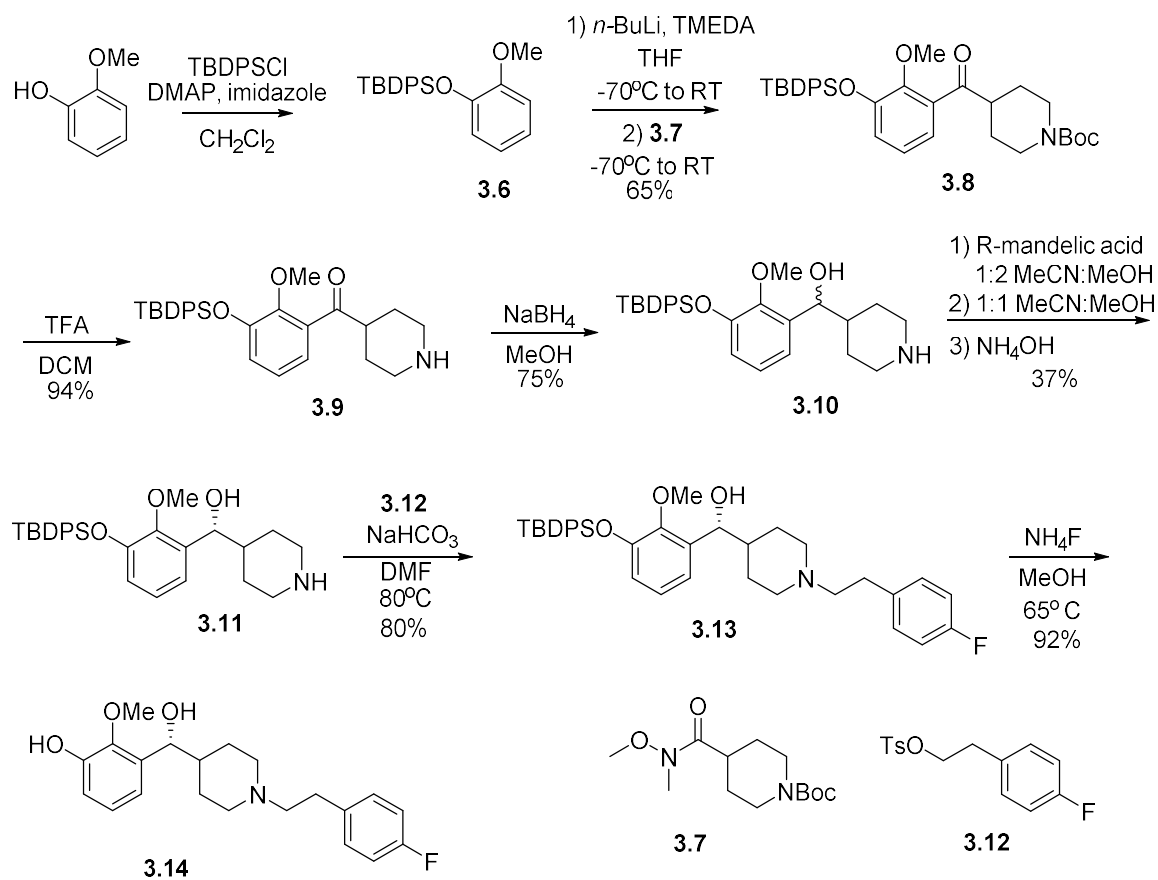
The alkyne needed for the joining of the two ligands via the CuAAC was then added using propargyl bromide, forming tertiary amine **3.4**. Deprotection of the hydroxyl group was then accomplished using tetrabutylammonium fluoride to give compound **3.5**.

3.2.2 Synthesis of M100907 Derivative

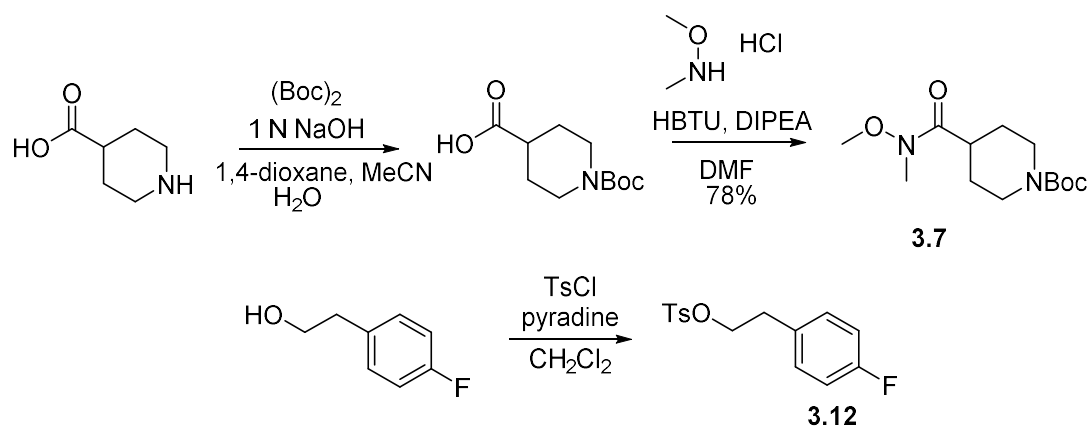
The 5-HT_{2A}R antagonist M100907 was selected over the 5-HT_{2C}R agonist WAY163909 as the pharmacophore of the bivalent ligand to which to add the functionalized linker. WAY163909 contains a secondary amine, which would need to be differentially protected before the amide coupling of the fluorophore to the linker.

M100907 could be synthesized according to the method reported by Rice⁴⁰ without the need for additional protection.

To synthesize the M100907 derivative, guaiacol was first protected as a silyl ether (**3.6**) and then coupled to Weinreb amide **3.7** to install the piperidine moiety (Scheme 3.3, 3.4). Deprotection of the amine and reduction of the ketone yielded racemic alcohol **3.10**. Chiral resolution was accomplished with (*R*)-mandelic acid according to the method reported by our group to give **3.11** as a single enantiomer.²⁸ The fluorine-substituted phenyl ring was added to yield **3.13**, which when deprotected gave **3.14**, a derivative of M100907.



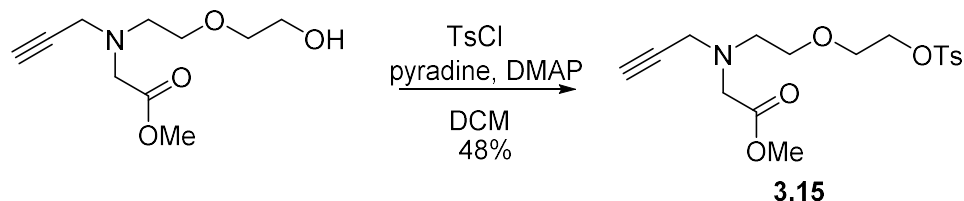
Scheme 3.3. Synthesis of a derivative of 5-HT_{2A}R antagonist M100907.



Scheme 3.4. Synthesis of compounds **3.7** and **3.12**.

3.2.3 Attachment of Functionalized Linker to M100907 Derivative

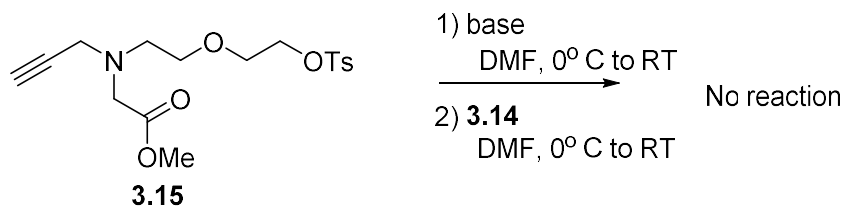
To attach the linker to M100907, the hydroxyl group was tosylated to form a leaving group (Scheme 3.5). The tosylation reaction proceeded in moderate yield, and unreacted starting material was recovered.



Scheme 3.5. Tosylation of tertiary amine.

Attempts to add the tosylated linker to M100907 were unsuccessful (Scheme 3.6). The first trial used sodium hydride as the base in dimethyl formamide, as these were the conditions used to add the non-functionalized PEG linker to M100907.²⁸ The procedure was repeated with potassium hexamethyldisilane (KHMDS). This base was chosen because of its different counterion and comparative ease of handling. The second attempt was also unsuccessful, indicating that a different leaving group may be necessary.

Leaving groups such as bromide, mesylate, or triflate could be added in one step from compound **3.5**.



Scheme 3.6. Attachment of tosylated linker to **3.14** was attempted with NaH and KHMDS as the base.

Chapter IV: Conclusion and Future Work

To functionalize the PEG linker of the bivalent ligand of M100907 and WAY163909, a linker (**3.5**) was synthesized containing a tertiary amine, which allowed for the inclusion of an ester side-chain. This ester is intended to be a handle for incorporation of a fluorophore via amide coupling, which will open the door to cellular imaging with this bivalent ligand and a greater understanding of the putative 5-HT_{2A}R/5-HT_{2C}R GPCR heterodimer. The use of a tertiary amine was shown to be more promising than the attempt to functionalize the linker at the triazole.

With the functionalized linker in hand, the next step is to add the functionalized linker to M100907. Use of the tosylate as the leaving group was shown to be ineffective, so other leaving groups should be tested, such as bromide and triflate. Once the linker is attached to M100907, the fluorophore can be added to the linker, and then the CuAAC can be used to join the compound with WAY163909. Biological imaging of the fluorophore-tagged bivalent ligand can be used to assess the selectivity for the 5-HT_{2A}R - 5-HT_{2C}R GPCR heterodimer over 5-HT_{2A}R and 5-HT_{2C}R monomers or homodimers, or to see if the ligand-receptor complex is internalized.

This functionalized linker, though developed for study of the 5-HT_{2A}R/5-HT_{2C}R heterodimer, would be compatible with any bivalent ligand that uses PEG as a tether in conjunction with the CuAAC. (In cases where the ligand has a free amine, such as the case of WAY163909, this may require additional protecting groups.) PEG is a commonly used tether due to its availability, flexibility, and hydrophilicity in comparison to a

hydrocarbon chain. Thus, the fluorophore-tagged tertiary amine linker is a general tool that can be used in the study of many different GPCR dimers.

Though the original intent of the functionalized linker was for the addition of a fluorophore, many other moieties can be added through the formation of an amide bond. In this sense, the linker can be used to make trivalent ligands. One possibility would be to add biotin to the bivalent ligand, which could be used with streptavidin to isolate the heterodimer. The azide, the alkyne, and the amide components of the trivalent ligand are all interchangeable, making this tertiary amine linker a truly versatile tool.

References

1. Santos, R.; Ursu, O.; Gaulton, A.; Bento, A. P.; Donadi, R. S.; Bologa, C. G.; Karlsson, A.; Al-Lazikani, B.; Hersey, A.; Oprea, T. I.; Overington, J. P. A comprehensive map of molecular drug targets. *Nature Reviews Drug Discovery* **2017**, *16* (1), 19-34.
2. Stadel, J. M.; Delean, A.; Lefkowitz, R. J. High-affinity agonist beta-adrenergic-receptor complex is an intermediate for catecholamine stimulation of adenylate-cyclase in turkey and frog erythrocyte-membranes. *Journal of Biological Chemistry* **1980**, *255* (4), 1436-1441.
3. O'Dowd, B. F.; Lefkowitz, R. J.; Caron, M. G. Structure of the adrenergic and related receptors. *Annual Review of Neuroscience* **1989**, *12*, 67-83.
4. Jones, K. A.; Borowsky, B.; Tamm, J. A.; Craig, D. A.; Durkin, M. M.; Dai, M.; Yao, W. J.; Johnson, M.; Gunwaldsen, C.; Huang, L. Y.; Tang, C.; Shen, Q. R.; Salon, J. A.; Morse, K.; Laz, T.; Smith, K. E.; Nagarathnam, D.; Noble, S. A.; Branchek, T. A.; Gerald, C. GABA(B) receptors function as a heteromeric assembly of the subunits GABA(B)R1 and GABA(B)R2. *Nature* **1998**, *396* (6712), 674-679.
5. Kuner, R.; Kohr, G.; Grunewald, S.; Eisenhardt, G.; Bach, A.; Kornau, H. C. Role of heteromer formation in GABA(B) receptor function. *Science* **1999**, *283* (5398), 74-77.
6. Szidonya, L.; Cserzo, M.; Hunyady, L. Dimerization and oligomerization of G-protein-coupled receptors: debated structures with established and emerging functions. *Journal of Endocrinology* **2008**, *196* (3), 435-453.
7. Canals, M.; Marcellino, D.; Fanelli, F.; Ciruela, F.; de Benedetti, P.; Goldberg, S. R.; Neve, K.; Fuxe, K.; Agnati, L. F.; Woods, A. S.; Ferre, S.; Lluís, C.; Bouvier, M.; Franco, R. Adenosine A(2A)-dopamine D2 receptor-receptor heteromerization - Qualitative and quantitative assessment by fluorescence and bioluminescence energy transfer. *Journal of Biological Chemistry* **2003**, *278* (47), 46741-46749.
8. Armentero, M. T.; Pinna, A.; Ferre, S.; Lanciego, J. L.; Muller, C. E.; Franco, R. Past, present and future of A(2A) adenosine receptor antagonists in the therapy of Parkinson's disease. *Pharmacology & Therapeutics* **2011**, *132* (3), 280-299.
9. Jenner, P. The MPTP-treated primate as a model of motor complications in PD - Primate model of motor complications. *Neurology* **2003**, *61* (6), S4-S11.
10. Zheng, Y.; Akgun, E.; Harikumar, K. G.; Hopson, J.; Powers, M. D.; Lunzer, M. M.; Miller, L. J.; Portoghese, P. S., Induced Association of mu Opioid (MOP) and Type 2 Cholecystinin (CCK2) Receptors by Novel Bivalent Ligands. *Journal of Medicinal Chemistry* **2009**, *52* (2), 247-258.

11. Hayashi, R.; Osada, S.; Yoshiki, M.; Sugiyama, D.; Fujita, I.; Hamasaki, Y.; Kodama, H. Superoxide production in human neutrophils is enhanced by treatment with transmembrane peptides derived from human formyl peptide receptor. *Journal of Biochemistry* **2006**, *139* (6), 981-988.
12. Erez, M.; Takemori, A. E.; Portoghese, P. S. Narcotic antagonistic potency of bivalent ligands which contain beta-naltrexamine - evidence for bridging between proximal recognition sites. *Journal of Medicinal Chemistry* **1982**, *25* (7), 847-849.
13. Portoghese, P. S.; Ronsisvalle, G.; Larson, D. L.; Yim, C. B.; Sayre, L. M.; Takemori, A. E. Opioid agonist and antagonist bivalent ligands as receptor probes. *Life Sciences* **1982**, *31* (12-1), 1283-1286.
14. McLellan, A. T.; Lewis, D. C.; O'Brien, C. P.; Kleber, H. D. Drug dependence, a chronic medical illness - Implications for treatment, insurance, and outcomes evaluation. *JAMA-Journal of the American Medical Association* **2000**, *284* (13), 1689-1695.
15. Moeller, F. G.; Dougherty, D. M.; Barratt, E. S.; Schmitz, J. M.; Swann, A. C.; Grabowski, J. The impact of impulsivity on cocaine use and retention in treatment. *Journal of Substance Abuse Treatment* **2001**, *21* (4), 193-198.
16. O'Brien, C. P.; Childress, A. R.; Ehrman, R.; Robbins, S. J. Conditioning factors in drug abuse: can they explain compulsion? *Journal of Psychopharmacology* **1998**, *12* (1), 15-22.
17. Winstanley, C. A.; Chudasama, Y.; Dalley, J. W.; Theobald, D. E. H.; Glennon, J. C.; Robbins, T. W. Intra-prefrontal S-OH-DPAT and M100907 improve visuospatial attention and decrease impulsivity on the five-choice serial reaction time task in rats. *Psychopharmacology* **2003**, *167* (3), 304-314.
18. Anastasio, N. C.; Stoffel, E. C.; Fox, R. G.; Bubar, M. J.; Rice, K. C.; Moeller, F. G.; Cunningham, K. A. Serotonin (5-hydroxytryptamine) 5-HT_{2A} receptor: association with inherent and cocaine-evoked behavioral disinhibition in rats. *Behavioural Pharmacology* **2011**, *22* (3), 248-261.
19. Fletcher, P. J.; Tampakeras, M.; Sinyard, J.; Higgins, G. A. Opposing effects of 5-HT_{2A} and 5-HT_{2C} receptor antagonists in the rat and mouse on premature responding in the five-choice serial reaction time test. *Psychopharmacology* **2007**, *195* (2), 223-234.
20. Navarra, R.; Comery, T. A.; Graf, R.; Rosenzweig-Lipson, S.; Day, M. The 5-HT_{2C} receptor agonist WAY-163909 decreases impulsivity in the 5-choice serial reaction time test. *Behavioural Brain Research* **2008**, *188* (2), 412-415.

21. Fletcher, P. J.; Rizos, Z.; Sinyard, J.; Tampakeras, M.; Higgins, G. A. The 5-HT_{2C} receptor agonist Ro60-0175 reduces cocaine self-administration and reinstatement induced by the stressor yohimbine, and contextual cues. *Neuropsychopharmacology* **2008**, *33* (6), 1402-1412.
22. Cunningham, K. A.; Anastasio, N. C.; Fox, R. G.; Stutz, S. J.; Bubar, M. J.; Swinford, S. E.; Watson, C. S.; Gilbertson, S. R.; Rice, K. C.; Rosenzweig-Lipson, S.; Moeller, F. G. Synergism between a serotonin 5-HT_{2A} receptor (5-HT_{2AR}) antagonist and 5-HT_{2CR} agonist suggests new pharmacotherapeutics for cocaine addiction. *ACS Chemical Neuroscience* **2013**, *4* (1), 110-121.
23. Moutkine, I.; Quentin, E.; Guiard, B. P.; Maroteaux, L.; Doly, S. Heterodimers of serotonin receptor subtypes 2 are driven by 5-HT_{2C} protomers. *Journal of Biological Chemistry* **2017**, *292* (15), 6352-6368.
24. Shashack, M. J.; Cunningham, K. A.; Seitz, P. K.; McGinnis, A.; Smith, T. D.; Watson, C. S.; Gilbertson, S. R. Synthesis and Evaluation of Dimeric Derivatives of 5-HT_{2A} Receptor (5-HT_{2AR}) Antagonist M-100907. *ACS Chemical Neuroscience* **2011**, *2* (11), 640-644.
25. Brea, J.; Castro, M.; Giraldo, J.; Lopez-Gimenez, J. F.; Padin, J. F.; Quintian, F.; Cadavid, M. I.; Vilaro, M. T.; Mengod, G.; Berg, K. A.; Clarke, W. P.; Vilaro, J. P.; Milligan, G.; Loza, M. I. Evidence for distinct antagonist-revealed functional states of 5-hydroxytryptamine(2A) receptor homodimers. *Molecular Pharmacology* **2009**, *75* (6), 1380-1391.
26. Teitler, M.; Klein, M. T. A new approach for studying GPCR dimers: Drug-induced inactivation and reactivation to reveal GPCR dimer function in vitro, in primary culture, and in vivo. *Pharmacology & Therapeutics* **2012**, *133* (2), 205-217.
27. Chen, Y. C.; Hartley, R. M.; Anastasio, N. C.; Cunningham, K. A.; Gilbertson, S. R. Synthesis and structure-activity relationships of tool compounds based on WAY163909, a 5-HT_{2C} receptor agonist. *ACS Chemical Neuroscience* **2017**, *8* (5), 1004-1010.
28. Chen, Y.C. Investigating the role of serotonin 2A and 2C receptors in neurobiology. University of Houston, Houston, Texas, 2015.
29. Wu, P. G.; Brand, L. Resonance energy-transfer - methods and applications. *Analytical Biochemistry* **1994**, *218* (1), 1-13.
30. Clayton, A. H. A.; Chattopadhyay, A. Taking care of bystander FRET in a crowded cell membrane environment. *Biophysical Journal* **2014**, *106* (6), 1227-1228.

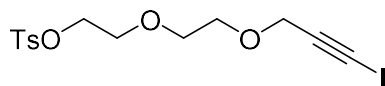
31. Herrick-Davis, K.; Grinde, E.; Lindsley, T.; Cowan, A.; Mazurkiewicz, J. E. Oligomer size of the serotonin 5-hydroxytryptamine 2C (5-HT_{2C}) receptor revealed by fluorescence correlation spectroscopy with photon counting histogram analysis: evidence for homodimers without monomers or tetramers. *Journal of Biological Chemistry* **2012**, *287* (28), 23604-23614.
32. Hern, J. A.; Baig, A. H.; Mashanov, G. I.; Birdsall, B.; Corrie, J. E. T.; Lazareno, S.; Molloy, J. E.; Birdsall, N. J. M. Formation and dissociation of M-1 muscarinic receptor dimers seen by total internal reflection fluorescence imaging of single molecules. *Proceedings of the National Academy of Sciences* **2010**, *107* (6), 2693-2698.
33. Kasai, R. S.; Suzuki, K. G. N.; Prossnitz, E. R.; Koyama-Honda, I.; Nakada, C.; Fujiwara, T. K.; Kusumi, A. Full characterization of GPCR monomer-dimer dynamic equilibrium by single molecule imaging. *Journal of Cell Biology* **2011**, *192* (3), 463-480.
34. Tanaka, T.; Nomura, W.; Narumi, T.; Masuda, A.; Tamamura, H. Bivalent Ligands of CXCR4 with Rigid Linkers for Elucidation of the Dimerization State in Cells. *Journal of the American Chemical Society* **2010**, *132* (45), 15899-15901.
35. Xu, L. P.; Josan, J. S.; Vagner, J.; Caplan, M. R.; Hruby, V. J.; Mash, E. A.; Lynch, R. M.; Morse, D. L.; Gillies, R. J. Heterobivalent ligands target cell-surface receptor combinations in vivo. *Proceedings of the National Academy of Sciences* **2012**, *109* (52), 21295-21300.
36. Hart, N. J.; Chung, W. J.; Weber, C.; Ananthkrishnan, K.; Anderson, M.; Patek, R.; Zhang, Z. Y.; Limesand, S. W.; Vagner, J.; Lynch, R. M. Hetero-bivalent GLP-1/glibenclamide for targeting pancreatic beta-cells. *ChemBioChem* **2014**, *15* (1), 135-145.
37. Nomura, W.; Aikawa, H.; Taketomi, S.; Tanabe, M.; Mizuguchi, T.; Tamamura, H. Exploration of labeling by near infrared dyes of the polyproline linker for bivalent-type CXCR4 ligands. *Bioorganic & Medicinal Chemistry* **2015**, *23* (21), 6967-6973.
38. Hein, J. E.; Tripp, J. C.; Krasnova, L. B.; Sharpless, K. B.; Fokin, V. V. Copper(I)-catalyzed cycloaddition of organic azides and 1-iodoalkynes. *Angewandte Chemie-International Edition* **2009**, *48* (43), 8018-8021.
39. AbdelMagid, A. F.; Carson, K. G.; Harris, B. D.; Maryanoff, C. A.; Shah, R. D. Reductive amination of aldehydes and ketones with sodium triacetoxyborohydride. Studies on direct and indirect reductive amination procedures. *Journal of Organic Chemistry* **1996**, *61* (11), 3849-3862.
40. Ullrich, T.; Rice, K. C. A practical synthesis of the serotonin 5-HT_{2A} receptor antagonist MDL 100907, its enantiomer and their 3-phenolic derivatives as precursors for C-11 labeled PET ligands. *Bioorganic & Medicinal Chemistry* **2000**, *8* (10), 2427-2432.

Chapter V: Experimental Section

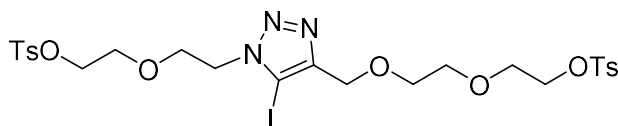
5.1 General Methods

All starting materials and reagents were purchased from Sigma-Aldrich, Acros, AstaTech, and Aapptec and unless noted were used without further purification. Thin-layer chromatography (TLC) was performed on Silicycle glass backed plates (extra hard layer, 250 mm thick, 60 Å, with F-254 indicator) and components were visualized by UV light (254 nm) and/or p-anisaldehyde, basic permanganate (KMnO₄) solution or ninhydrin solution. Flash column chromatography was performed using Silicycle silica gel (particle size 40-63 μm, 230-400 mesh). NMR spectra were obtained using JEOL ECX-400 spectrometer (400 MHz for ¹H NMR and 101 MHz for ¹³C NMR), JEOL ECA-500 spectrometer (500 MHz for ¹H NMR and 126 MHz for ¹³C NMR), or JEOL ECA-600 spectrometer (600 MHz for ¹H NMR and 151 MHz for ¹³C NMR). Chemical shifts were referenced to the residual chloroform-H peak at 7.26 ppm (¹H) and 77 ppm (¹³C) in CDCl₃. Chemical shifts were reported in parts per million (ppm, δ). Multiplicity were indicated as s for singlet, d for doublet, t for triplet, q for quartet, m for multiplet, br for broad resonance and the coupling constants (J) were reported in Hz.

5.2 Experimental Procedures

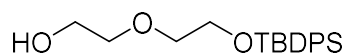


2-(2-(3-iodoprop-2-ynoxy)ethoxy)ethyl 4-methylbenzenesulfonate (2.5): 2-(2-(prop-2-ynoxy)ethoxy)ethyl 4-methylbenzenesulfonate (959 mg, 3.2 mmol) was dissolved in anhydrous THF (8 mL). Copper iodide (30 mg, 0.16 mmol) and N-iodomorpholine hydriodide (1.193 g, 3.5 mmol) were added. The reaction was stirred at room temperature under a nitrogen atmosphere for two hours, forming a white precipitate. The reaction mixture was filtered through celite and rinsed with DCM. Concentration under reduced pressure yielded the crude product as a brown oil. Purification attempts were unsuccessful.

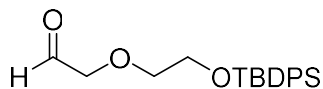


2-(2-((5-iodo-1-(2-(2-(tosyloxy)ethoxy)ethyl)-1H-1,2,3-triazol-4-yl)methoxy)ethoxy)ethyl 4-methylbenzenesulfonate (2.6): Copper iodide (6 mg, 0.03 mmol) and triethylamine (61 mg, 0.6 mmol) were stirred together in THF (2 mL), forming a blue-green solution. Crude 2-(2-(3-iodoprop-2-ynoxy)ethoxy)ethyl 4-methylbenzenesulfonate (approximately 127 mg, 0.3 mmol) was dissolved in THF (1.5 mL) and added to the reaction mixture. 2-(2-azidoethoxy)ethyl 4-methylbenzenesulfonate (86 mg, 0.4 mmol) was dissolved in THF (1.5 mL) and added to the reaction mixture.

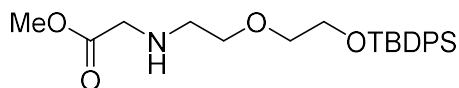
The reaction was stirred at room temperature under a nitrogen atmosphere for two hours. The reaction was quenched with 0.5 mL of saturated ammonium hydroxide. The volatile components were removed under reduced pressure. The reaction mixture was suspended in water and diethyl ether and stirred for 20 minutes. The reaction mixture was extracted three times with diethyl ether. The organic layers were combined and dried with sodium sulfate. Filtration and concentration under reduced pressure yielded the crude product. Purification attempts were unsuccessful.



2-(2-(tert-butyldiphenylsilyloxy)ethoxy)ethanol (3.1): Diethylene glycol (6.00 g, 56.6 mmol) was added to a flame-dried round-bottom flask. Anhydrous DCM (38 mL) was added, then *tert*-butyldiphenylsilyl chloride (2.198 g, 8.0 mmol), imidazole (1.362 g, 20 mmol), and DMAP (20 mg, 0.16 mmol). The reaction was stirred at room temperature under an atmosphere of nitrogen for 22 hours. The reaction mixture was quenched with water and extracted with DCM. The organic layers were combined and dried with sodium sulfate. Filtration and concentration under reduced pressure yielded the crude product, which was purified by column chromatography (30% ethyl acetate in hexanes) to afford the product as a colorless oil (2.180 g, 79% yield). ¹H NMR (500 MHz, CDCl₃) δ 7.69 (dd, J = 7.8, 1.5 Hz, 4H), 7.46 – 7.36 (m, 6H), 3.83 – 3.79 (m, 2H), 3.71 (dd, J = 9.4, 5.6 Hz, 2H), 3.64 – 3.57 (m, 4H), 2.20 (t, J = 6.2 Hz, 1H), 1.05 (s, 9H). ¹³C NMR (126 MHz, CDCl₃) δ 135.70, 133.60, 129.80, 127.78, 72.47, 72.29, 63.61, 62.02, 26.89, 19.28.

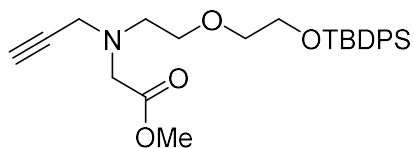


2-(2-(tert-butyl-diphenylsilyloxy)ethoxy)acetaldehyde (3.2): 2-(2-(tert-butyl-diphenylsilyloxy)ethoxy)ethanol (1.912 g, 5.6 mmol) was dissolved in DCM and placed in an ice bath for fifteen minutes. TEMPO (9.4 mg, 0.06 mmol) was added. Sodium bromide (628 mg, 6.1 mmol) was dissolved in saturated, aqueous sodium bicarbonate (28 mL), and the solution was added to the reaction mixture. Sodium hypochlorite (10-15% aqueous solution, 3.3 mL) was added dropwise, and the reaction mixture turned a light brown color. The ice bath was removed, and the reaction was stirred at room temperature for three hours, at which point the reaction mixture had turned white. The reaction mixture was extracted with DCM. The organic layers were combined and dried with sodium sulfate. Filtration and concentration under reduced pressure yielded the crude product, which was purified by column chromatography (20% ethyl acetate in hexanes) to afford the product as a colorless oil (1.578 g, 83% yield). ¹H NMR (400 MHz, CDCl₃) δ 9.71 (t, 1H), 7.76 – 7.60 (m, 4H), 7.49 – 7.32 (m, 6H), 4.15 (d, J = 0.7 Hz, 2H), 3.85 (dd, J = 5.4, 4.4 Hz, 2H), 3.68 (dd, J = 5.5, 4.3 Hz, 2H), 1.05 (s, 9H). ¹³C NMR (151 MHz, CDCl₃) δ 201.26, 135.68, 133.47, 129.83, 127.80, 76.95, 73.22, 63.62, 26.89, 19.26. LC-MS Calculated for C₂₀H₂₆O₃Si [M+H]⁺ 343; found: 343.

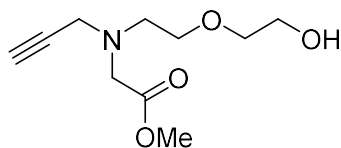


Methyl 2,2-dimethyl-3,3-diphenyl-4,7-dioxa-10-aza-3-siladodecan-12-oate (3.3):

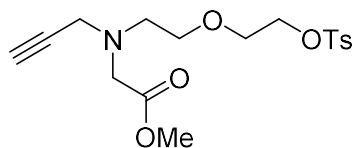
Glycine methyl ester hydrochloride (904 mg, 7.2 mmol), triethylamine (729 mg, 7.2 mmol), and anhydrous dichloromethane (55 mL) were added to an evaporation flask and mixed using a syringe. The mixture was added to 2-(2-(tert-butylidiphenylsilyloxy)ethoxy)acetaldehyde (1.875 g, 5.5 mmol). Sodium triacetoxyborohydride (3497 mg, 16.5 mmol) was added in four portions over one hour. The reaction was stirred at room temperature under nitrogen for 18 hours. The reaction was quenched with water and extracted with dichloromethane. The organic layers were combined and dried with sodium sulfate. Filtration and concentration under reduced pressure yielded the crude product, which was purified by column chromatography (100% ethyl acetate) to afford the product as a colorless oil (1.501 g, 66% yield). ¹H NMR (500 MHz, CDCl₃) δ 7.72 – 7.65 (m, 4H), 7.45 – 7.35 (m, 6H), 3.81 (t, 2H), 3.71 (s, 3H), 3.61 – 3.55 (m, 4H), 3.45 (s, 2H), 2.78 (t, 2H), 1.05 (s, 9H). ¹³C NMR (126 MHz, CDCl₃) δ 172.79, 135.70, 133.77, 129.70, 127.73, 72.33, 70.77, 63.48, 51.86, 50.96, 49.05, 26.89, 19.29. LC-MS Calculated for C₂₃H₃₃NO₄Si [M+H]⁺: 416; found: 416.



Methyl 2,2-dimethyl-3,3-diphenyl-10-(prop-2-ynyl)-4,7-dioxa-10-aza-3-siladodecan-12-oate (3.4): Methyl 2,2-dimethyl-3,3-diphenyl-4,7-dioxa-10-aza-3-siladodecan-12-oate (703 mg, 1.7 mmol) was dissolved in acetone (17 mL). Potassium carbonate (235 mg, 1.7 mmol) and propargyl bromide solution (80 weight percent in toluene, 0.21 mL, 1.9 mmol) were added to the reaction mixture. The reaction was stirred under nitrogen at room temperature for 18 hours. The reaction was quenched with water and extracted with dichloromethane. The organic layers were combined and dried with sodium sulfate. Filtration and concentration under reduced pressure yielded the crude product, which was purified by column chromatography (20% ethyl acetate in hexanes) to afford the product as a slightly yellow-tinted oil (590 mg, 77% yield). ¹H NMR (500 MHz, CDCl₃) δ 7.81 – 7.56 (m, 4H), 7.45 – 7.35 (m, 6H), 3.78 (t, J = 5.2 Hz, 2H), 3.68 (s, 3H), 3.64 (t, J = 5.6 Hz, 2H), 3.60 (d, J = 2.3 Hz, 2H), 3.55 (dd, J = 9.6, 4.5 Hz, 2H), 3.50 (s, 2H), 2.83 (t, J = 5.5 Hz, 2H), 2.22 (t, J = 2.3 Hz, 1H), 1.04 (s, 9H). ¹³C NMR (126 MHz, CDCl₃) δ 171.53, 135.70, 133.74, 129.70, 127.74, 78.76, 73.45, 72.37, 70.26, 63.44, 55.02, 53.30, 51.73, 43.85, 26.89, 19.27. LC-MS Calculated for C₂₆H₃₅NO₄Si [M+H]⁺: 454; found: 454.



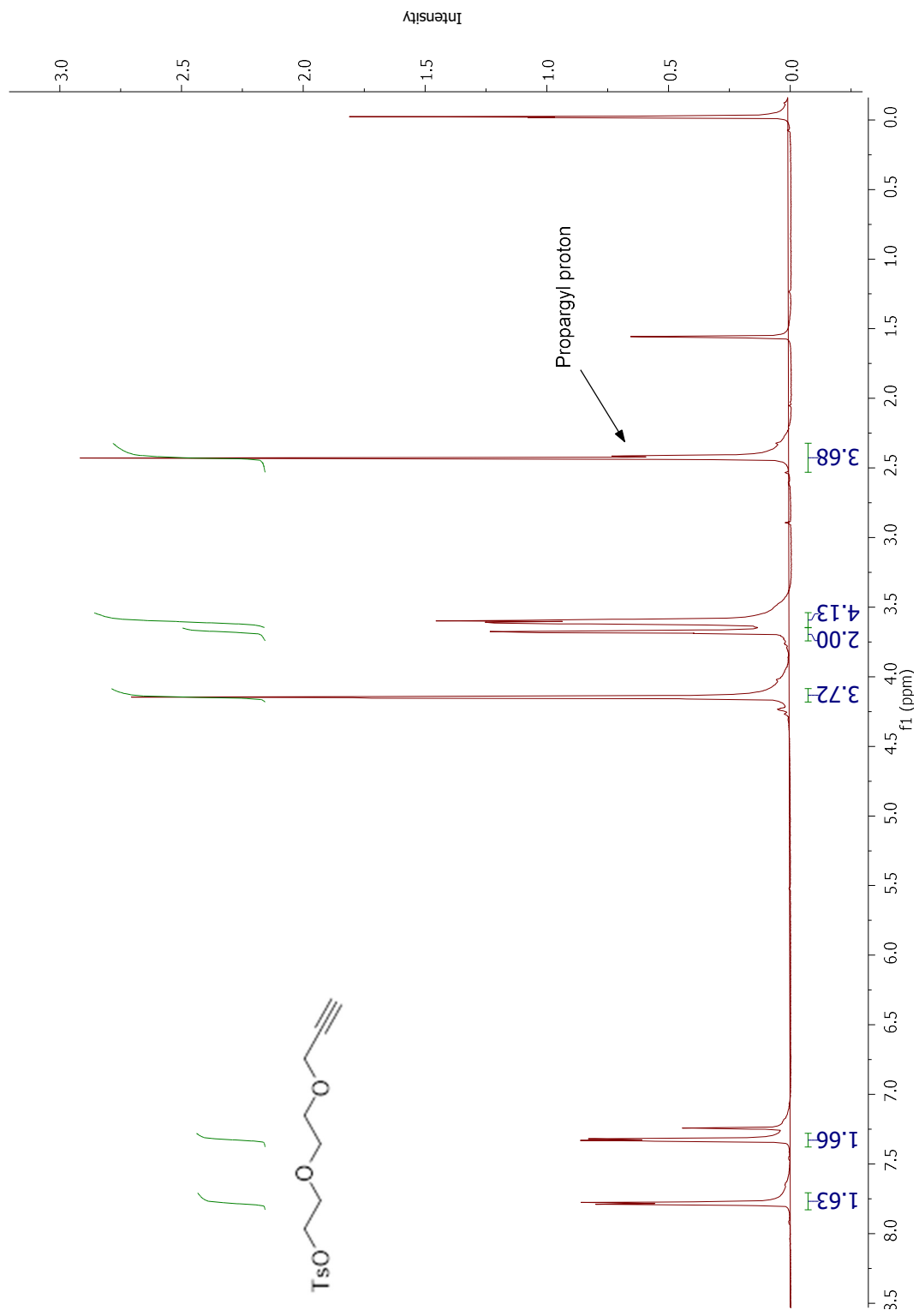
Methyl 2-((2-(2-hydroxyethoxy)ethyl)(prop-2-ynyl)amino)acetate (3.5): Methyl 2,2-dimethyl-3,3-diphenyl-10-(prop-2-ynyl)-4,7-dioxa-10-aza-3-siladodecan-12-oate (590 mg, 1.3 mmol) was dissolved in anhydrous tetrahydrofuran (13 mL). The reaction mixture was cooled in an ice bath for 20 minutes. Tetrabutylammonium fluoride (1.0 M in tetrahydrofuran, 2.0 mmol) was added to the reaction mixture. The reaction was removed from ice at stirred under nitrogen at room temperature for 24 hours. The reaction was quenched with water and extracted with dichloromethane. The organic layers were combined and dried with sodium sulfate. Filtration and concentration under reduced pressure yielded the crude product, which was purified by column chromatography (6% methanol in dichloromethane) to afford the product as a brownish oil (241 mg, 86% yield). $^1\text{H NMR}$ (500 MHz, CDCl_3) δ 3.75 – 3.69 (m, 5H), 3.66 (dd, $J = 12.2, 6.9$ Hz, 2H), 3.61 (d, $J = 2.4$ Hz, 2H), 3.57 (dd, $J = 5.9, 3.1$ Hz, 2H), 3.49 (s, 2H), 2.90 – 2.83 (m, 2H), 2.25 (t, $J = 2.3$ Hz, 1H), 1.75 (s, 1H). $^{13}\text{C NMR}$ (151 MHz, CDCl_3) δ 171.48, 78.42, 73.69, 72.42, 69.30, 61.94, 54.95, 53.22, 51.90, 43.65. LC-MS Calculated for $\text{C}_{10}\text{H}_{17}\text{NO}_4$ $[\text{M}+\text{H}]^+$: 216; found: 216.



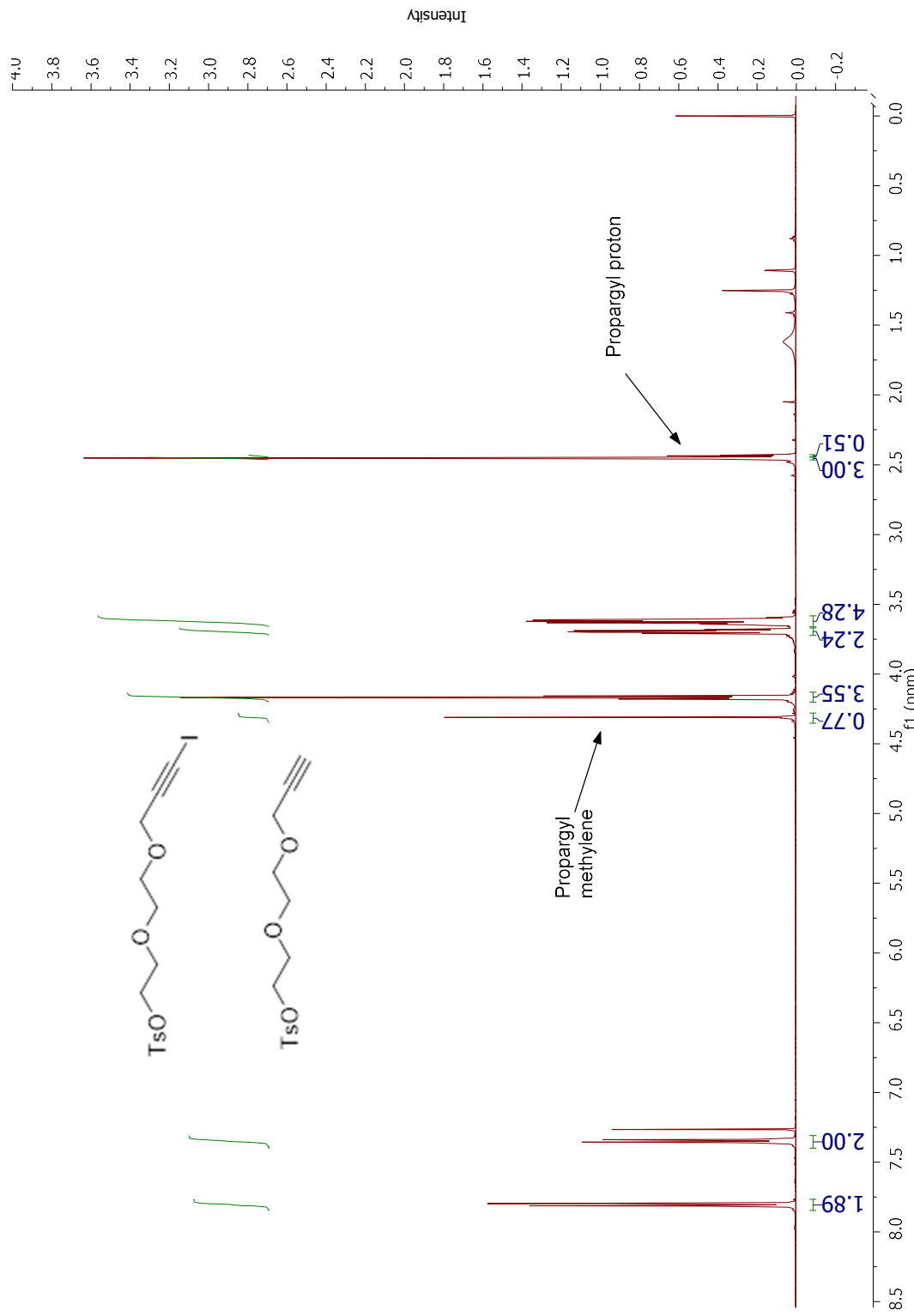
Methyl 2-(prop-2-ynyl(2-(2-(tosyloxy)ethoxy)ethyl)amino)acetate (3.15): Methyl 2-((2-(2-hydroxyethoxy)ethyl)(prop-2-ynyl)amino)acetate (241 mg, 1.1 mmol) was dissolved in anhydrous dichloromethane (11 mL). The reaction mixture was cooled in an ice bath for 20 minutes. Triethylamine (172 mg, 1.7 mmol) and dimethylaminopyridine (6 mg, 0.05 mmol) were added to the reaction mixture. *p*-Toluenesulfonyl chloride (324 mg, 1.7 mmol) was added portionwise over 15 minutes. The reaction mixture was removed from the ice bath and was stirred under nitrogen at room temperature for 24 hours. The reaction was quenched with water and extracted with dichloromethane. The organic layers were combined and dried with sodium sulfate. Filtration and concentration under reduced pressure yielded the crude product, which was purified by column chromatography (1% methanol in dichloromethane) to afford the product as a white foam (198 mg, 48%). ¹H NMR (400 MHz, CDCl₃) δ 7.73 (d, *J* = 8.1 Hz, 2H), 7.15 (d, *J* = 7.9 Hz, 2H), 4.99 – 4.86 (m, 4H), 4.20 – 4.07 (m, 4H), 4.07 – 3.98 (m, 2H), 3.95 – 3.85 (m, 2H), 3.76 (s, 3H), 2.99 (t, *J* = 2.4 Hz, 1H), 2.34 (s, 3H). ¹³C NMR (151 MHz, CDCl₃) δ 165.02, 143.65, 139.53, 128.78, 125.85, 83.24, 70.54, 60.30, 58.31, 56.81, 53.37, 51.36, 21.33. The signals at 60.30 and 58.31 ppm each represent two carbons, as indicated on the HMQC spectrum. LC-MS Calculated for C₁₇H₂₃NO₆S [M+H]⁺: 370; found: 370.

5.3 NMR Spectra

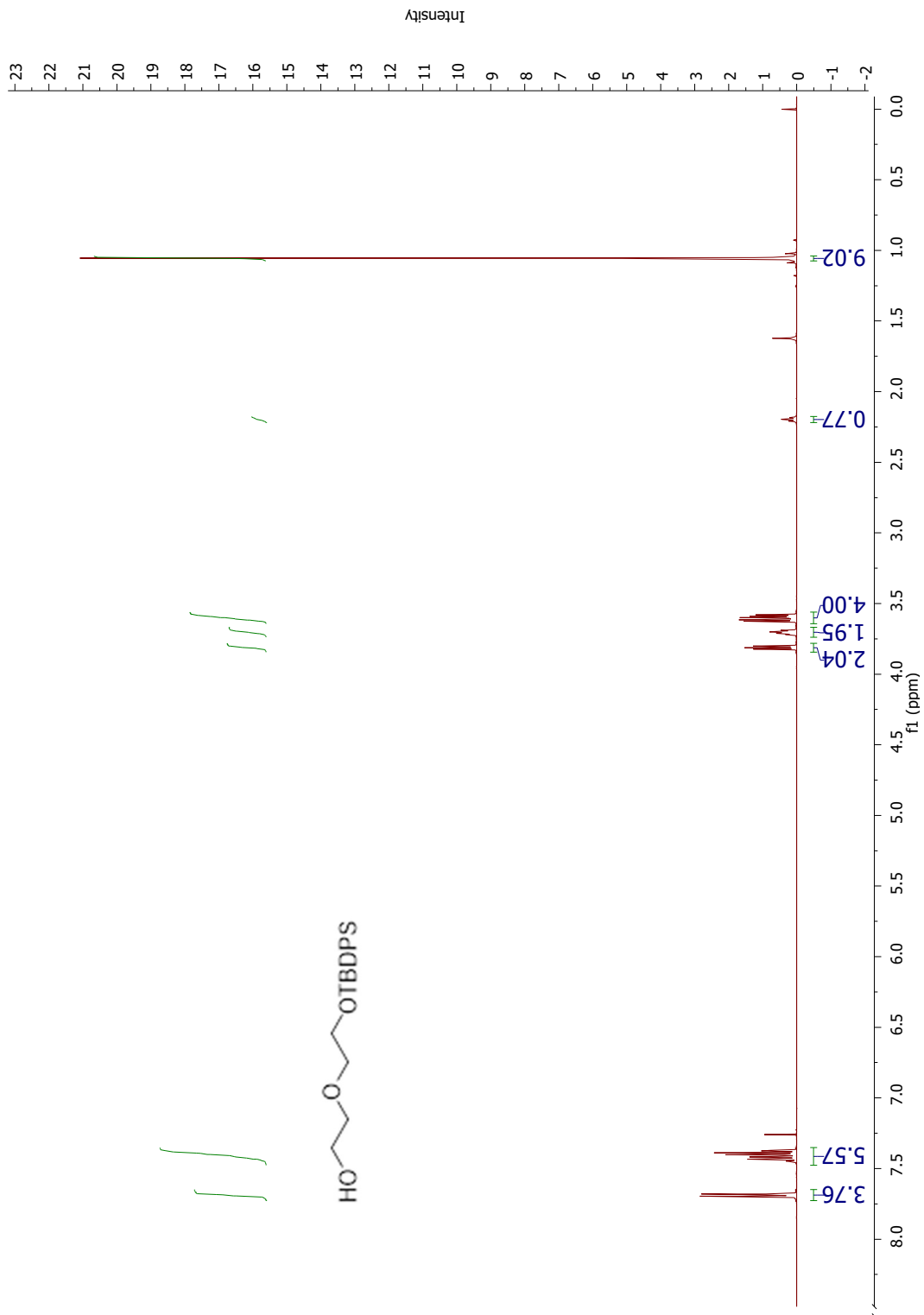
For the following NMR spectra, the horizontal axis represents the chemical shift in ppm, and the vertical axis represents signal intensity (a unitless quantity).



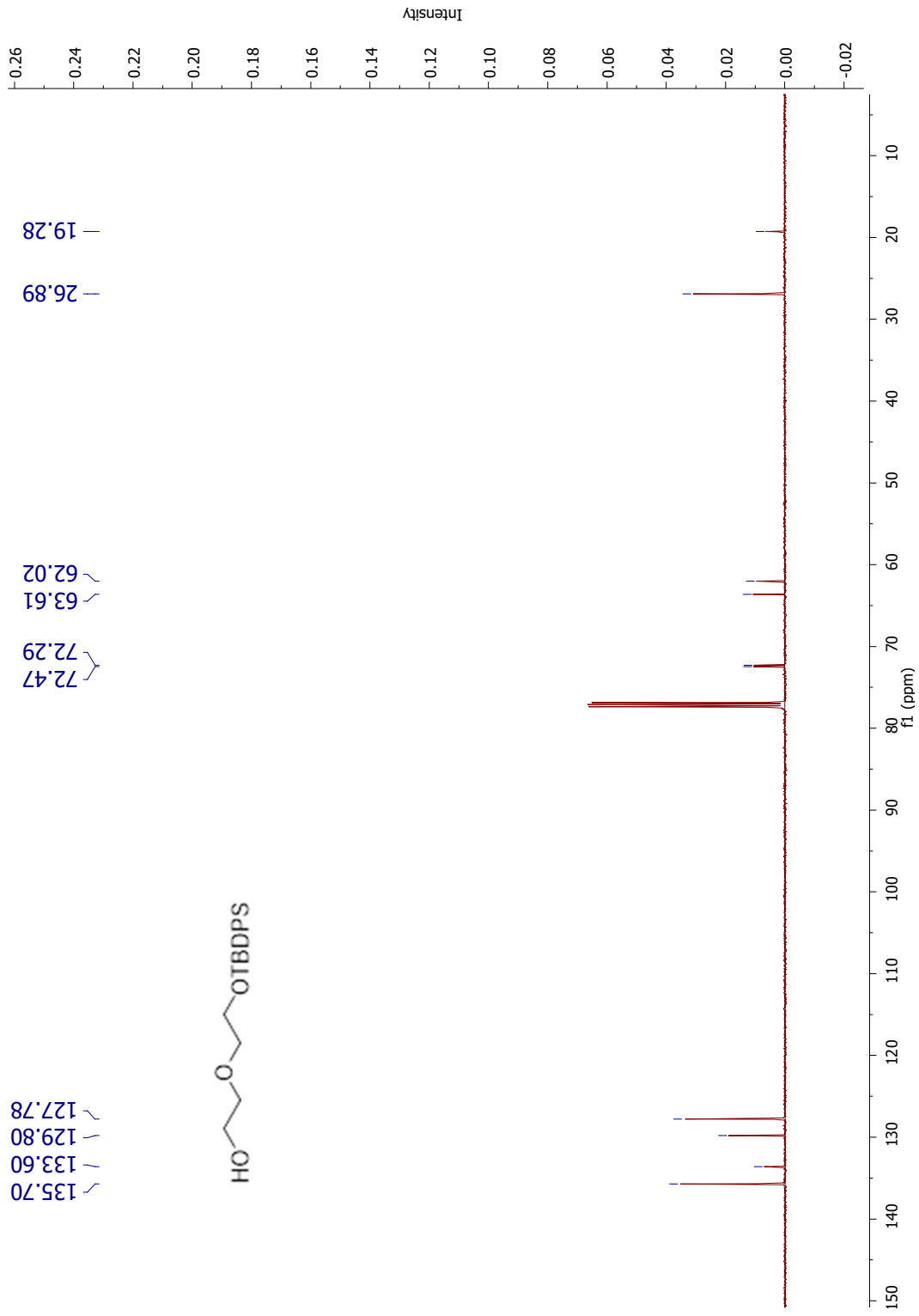
¹H NMR: 2-(2-(prop-2-ynoxy)ethoxy)ethyl 4-methylbenzenesulfonate (2.4)

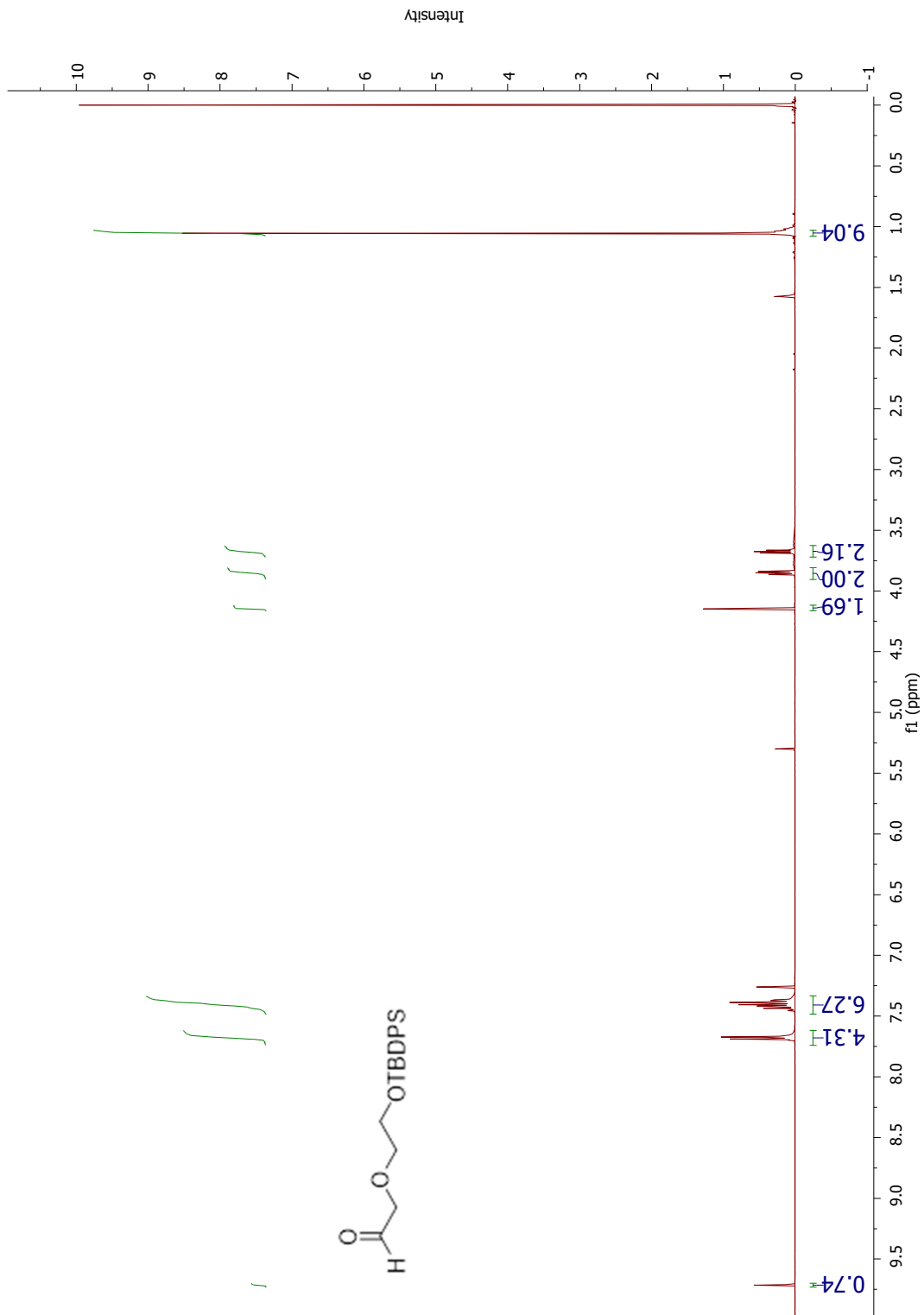
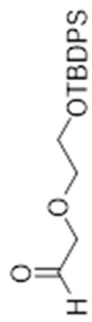


¹H NMR: 2-(2-(3-iodoprop-2-yn-1-yloxy)ethoxy)ethyl 4-methylbenzenesulfonate (2.5), which could not be separated cleanly from 2.4

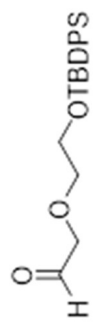
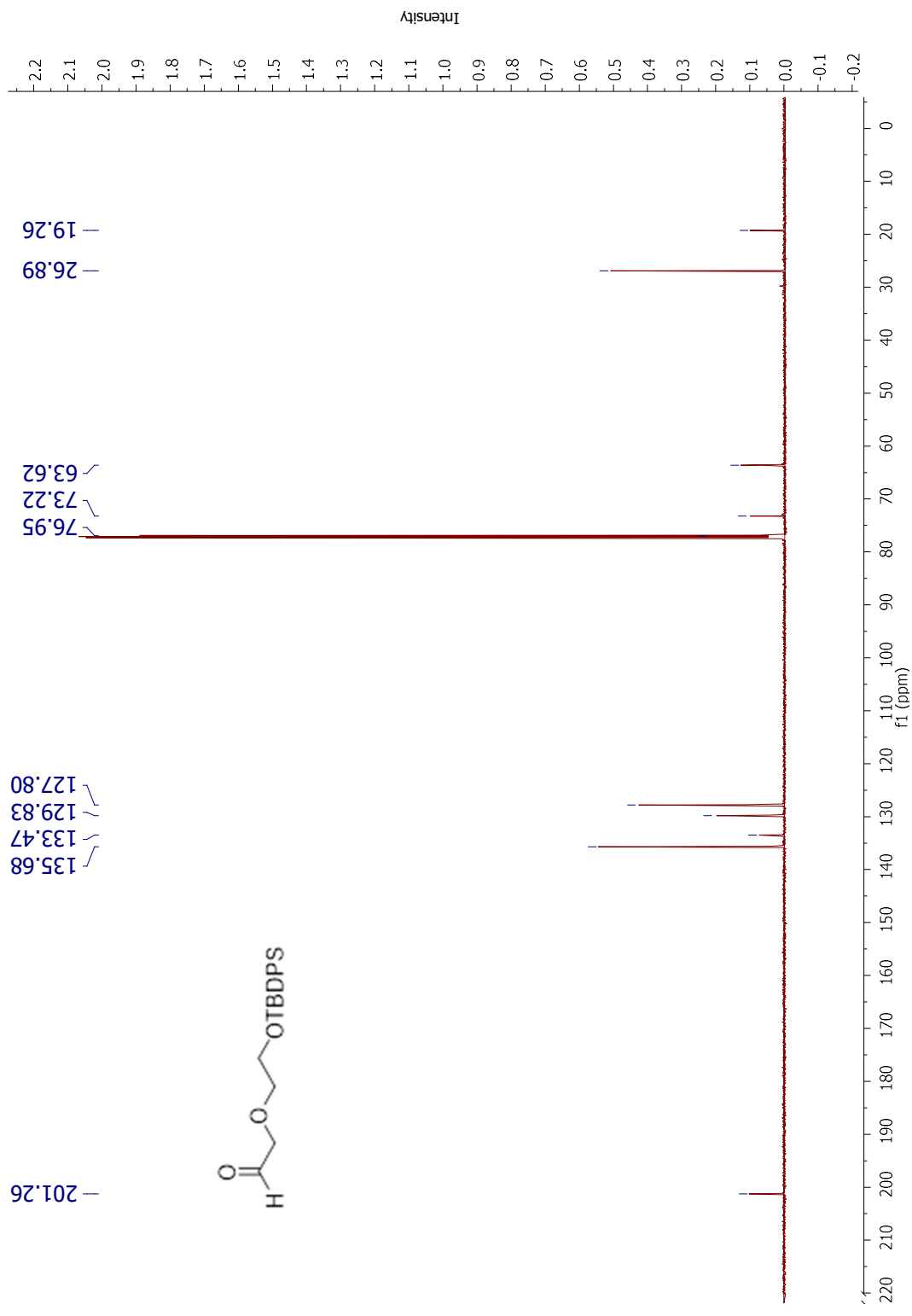


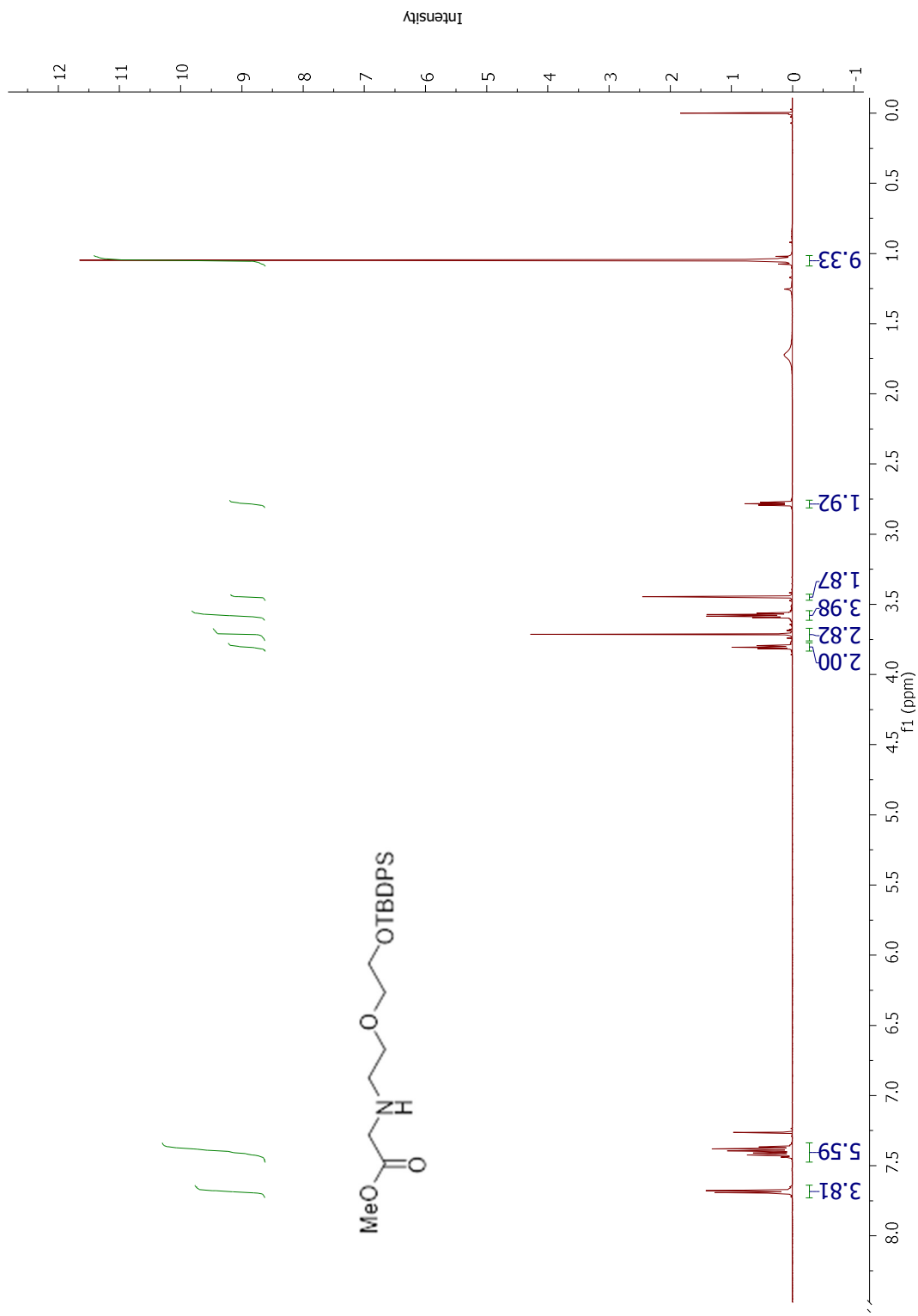
¹H NMR: 2-(2-(tert-butyl)diphenylsilyloxy)ethanol (3.1)



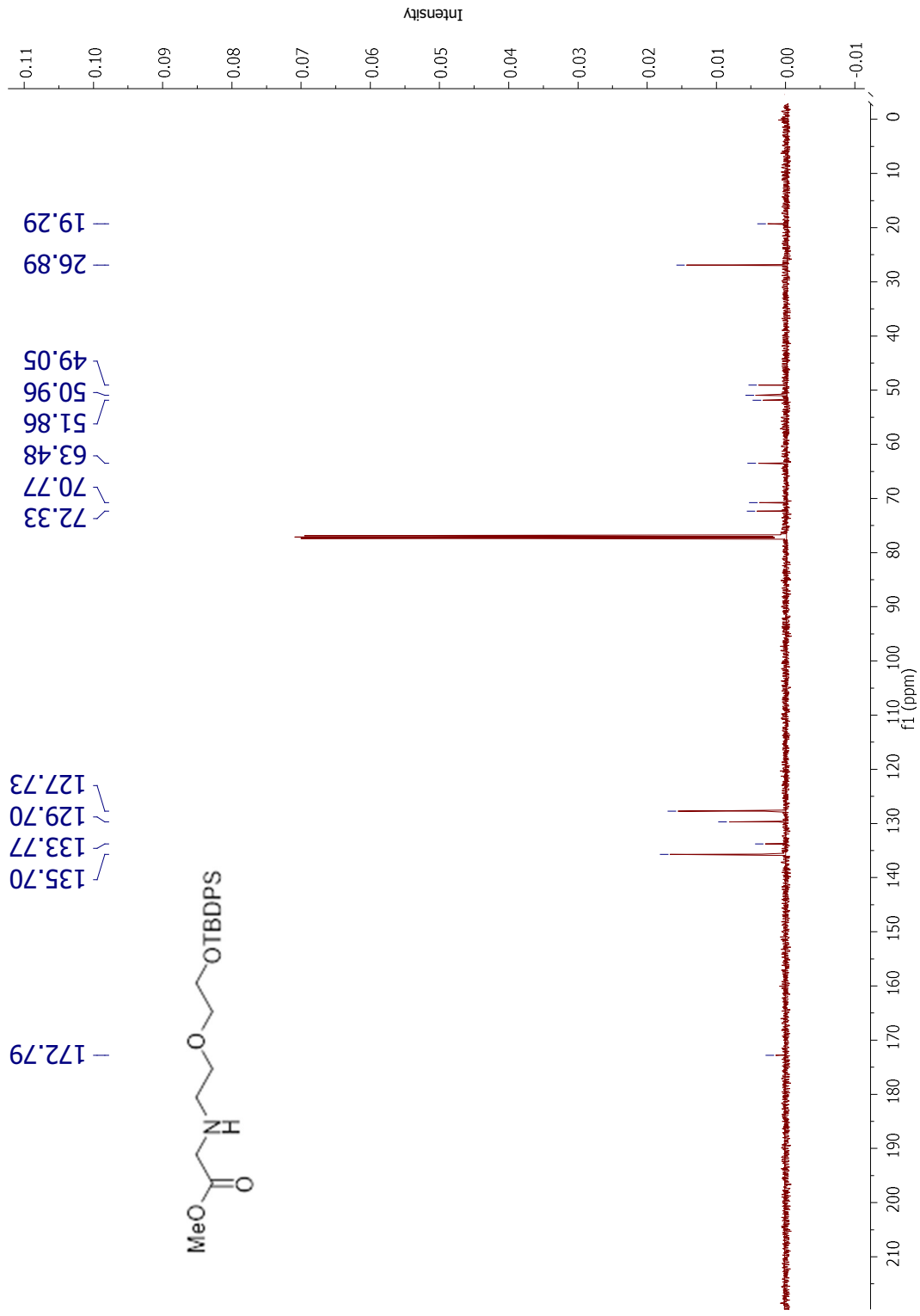


¹H NMR: 2-(2-(tert-butyl)diphenylsilyloxy)ethoxy)acetaldehyde (3.2)

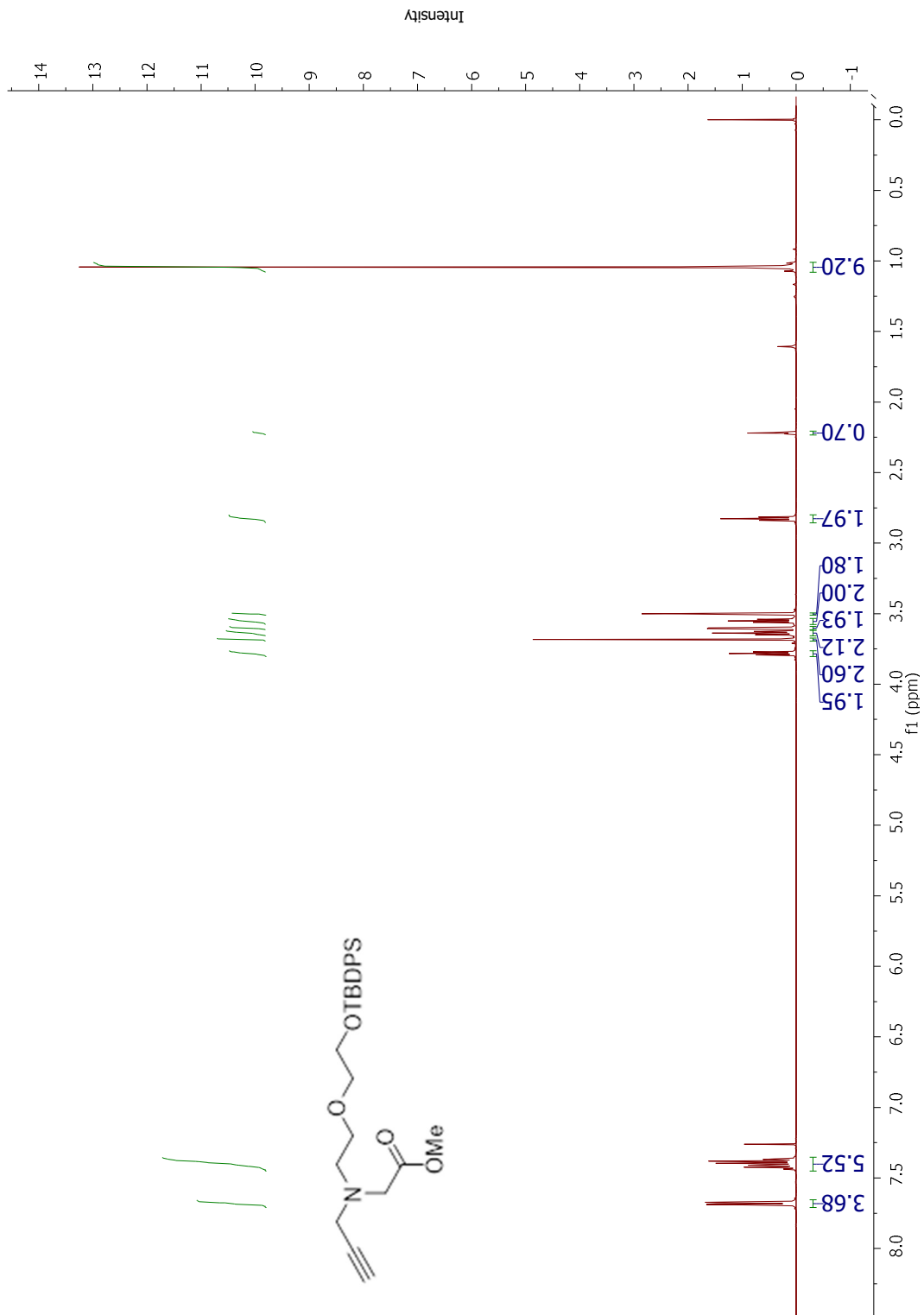




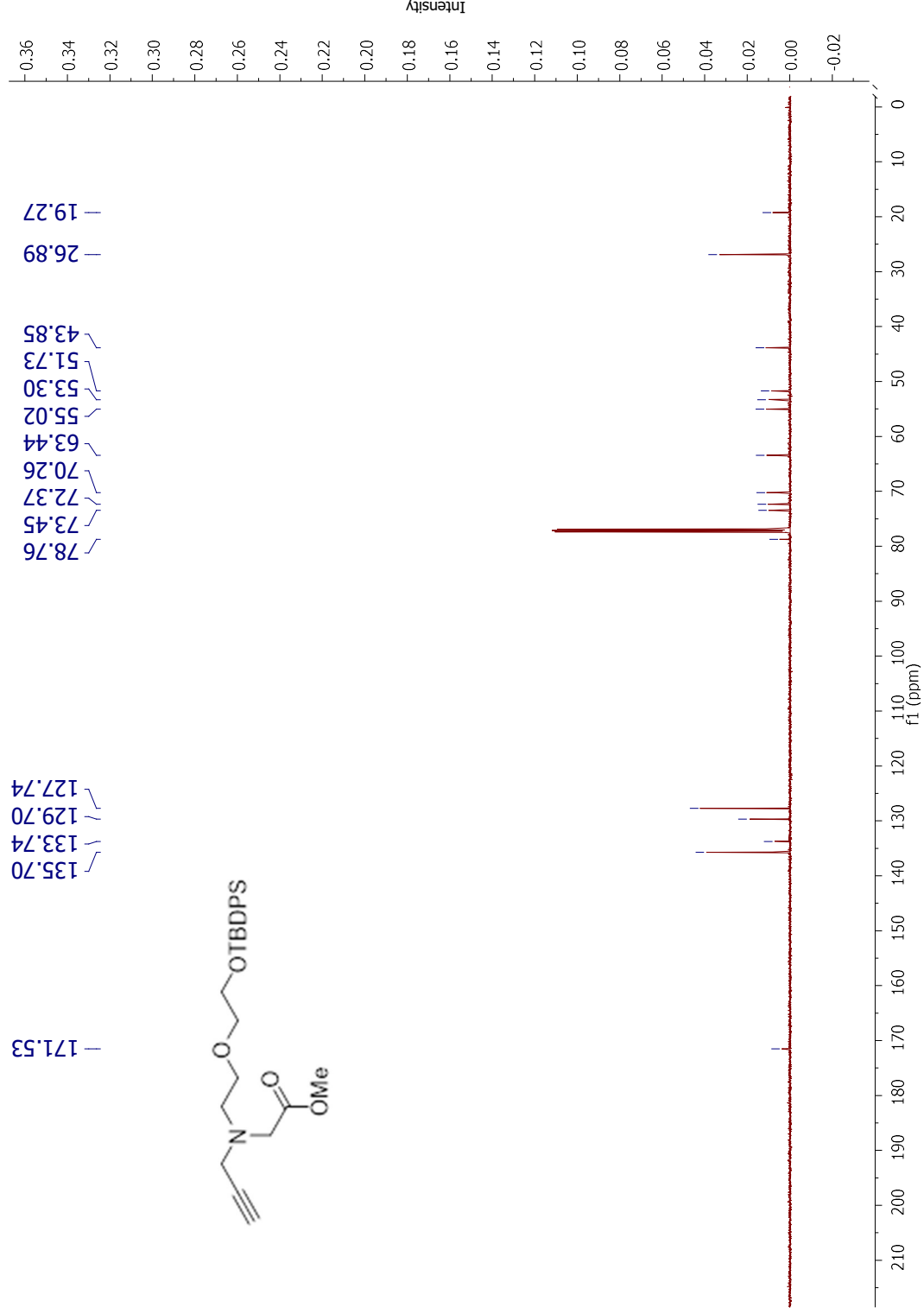
¹H NMR: Methyl 2,2-dimethyl-3,3-diphenyl-4,7-dioxo-10-aza-3-siladodecan-12-oate (3.3)



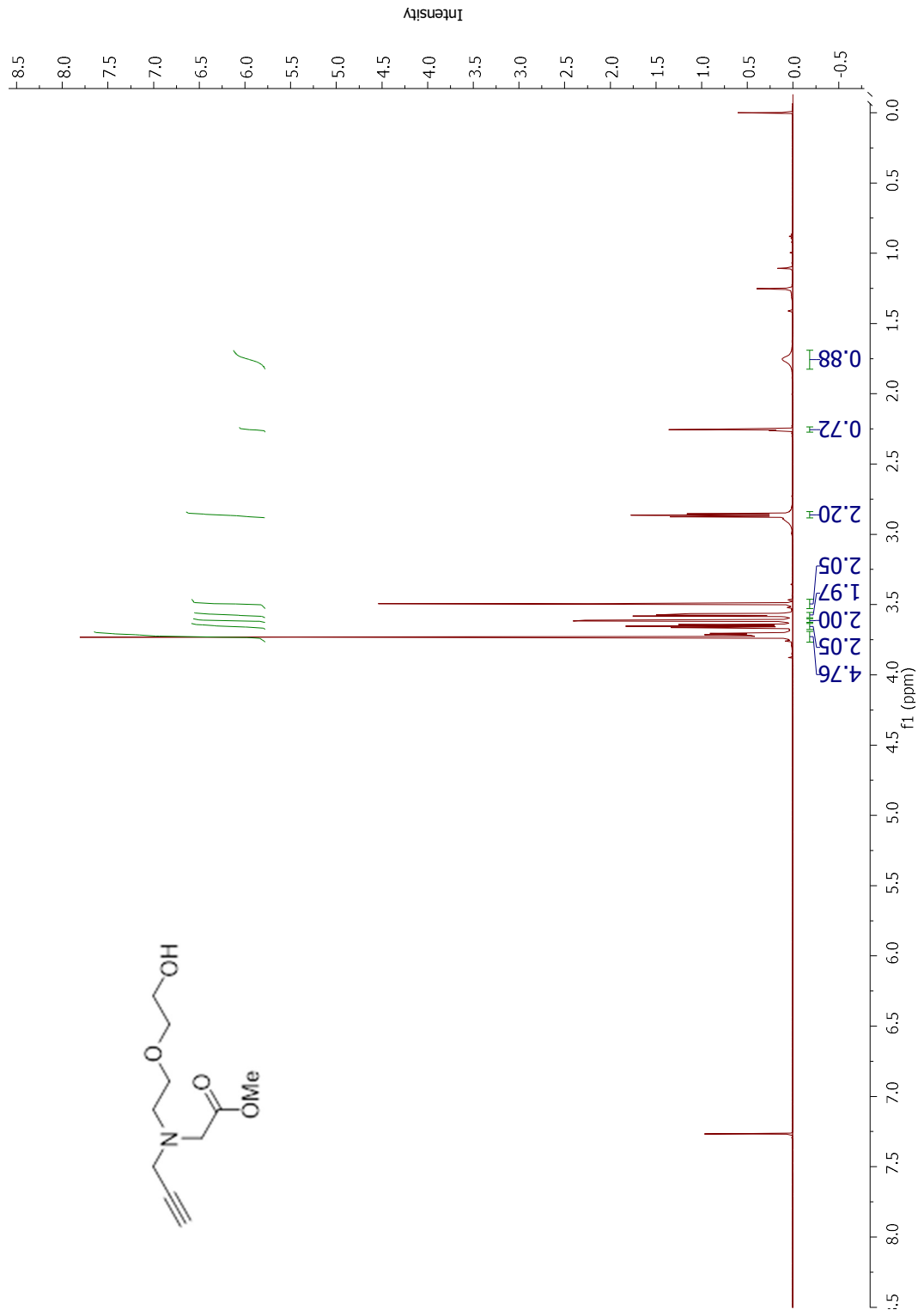
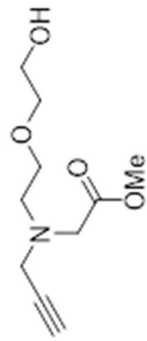
¹³C NMR: Methyl 2,2-dimethyl-3,3-diphenyl-4,7-dioxo-10-aza-10-aza-3-siladodecan-12-oate (3.3)



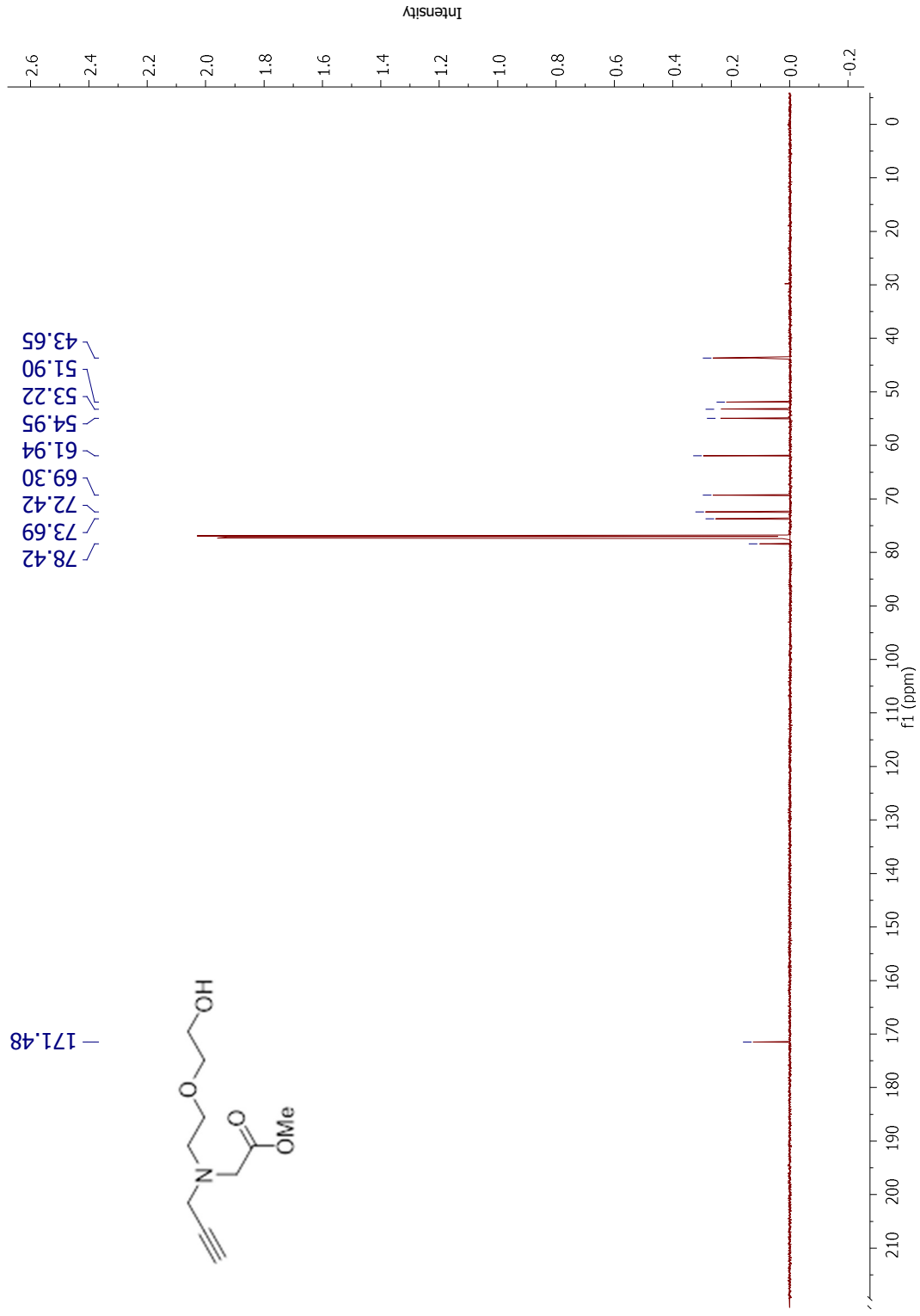
¹H NMR: Methyl 2,2-dimethyl-3,3-diphenyl-10-(prop-2-ynyl)-4,7-dioxa-10-aza-3-siladodecan-12-oate (**3.4**)

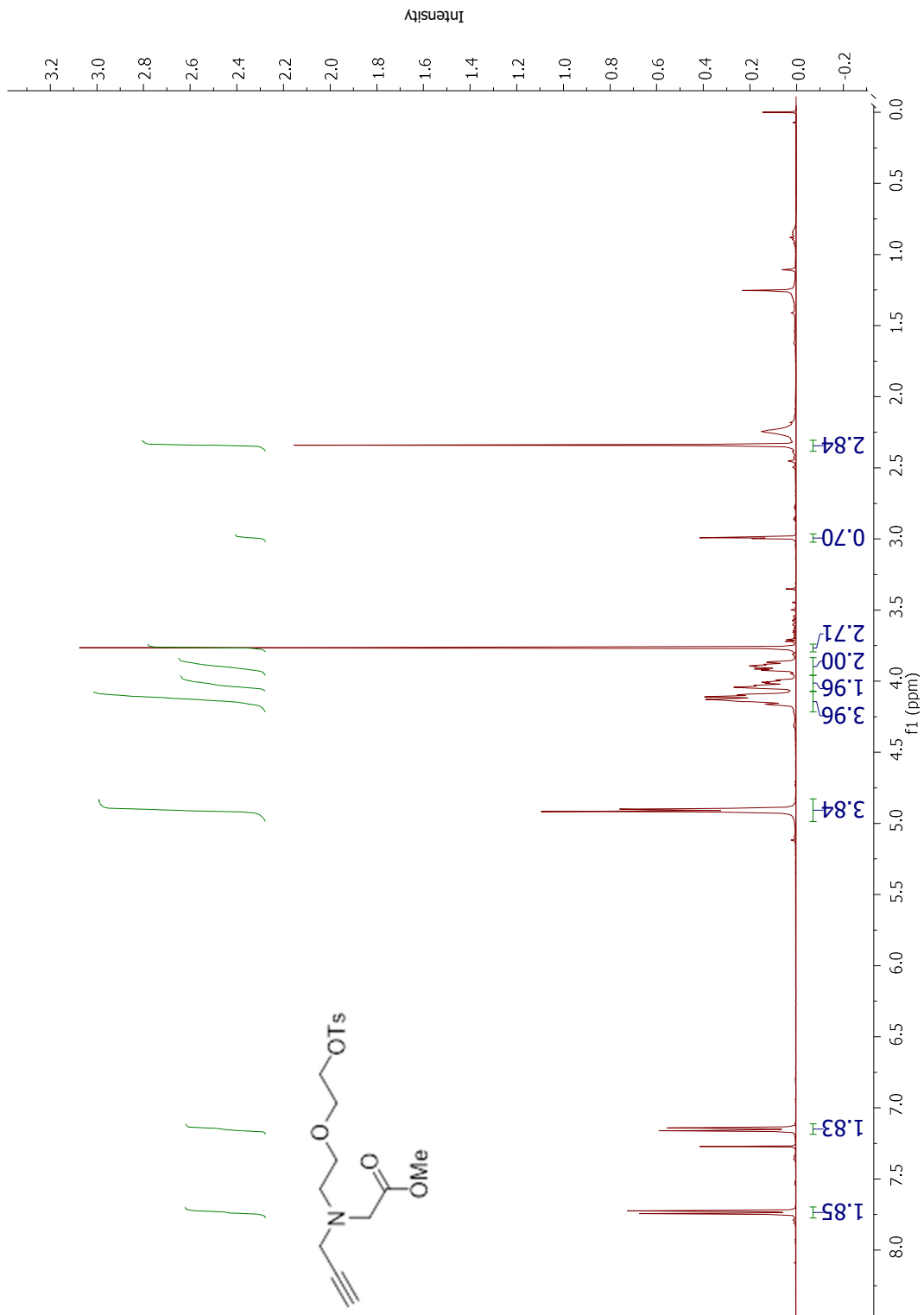


¹³C NMR: Methyl 2,2-dimethyl-3,3-diphenyl-10-(prop-2-ynyl)-4,7-dioxo-10-aza-3-siladodecan-12-oate (3.4)

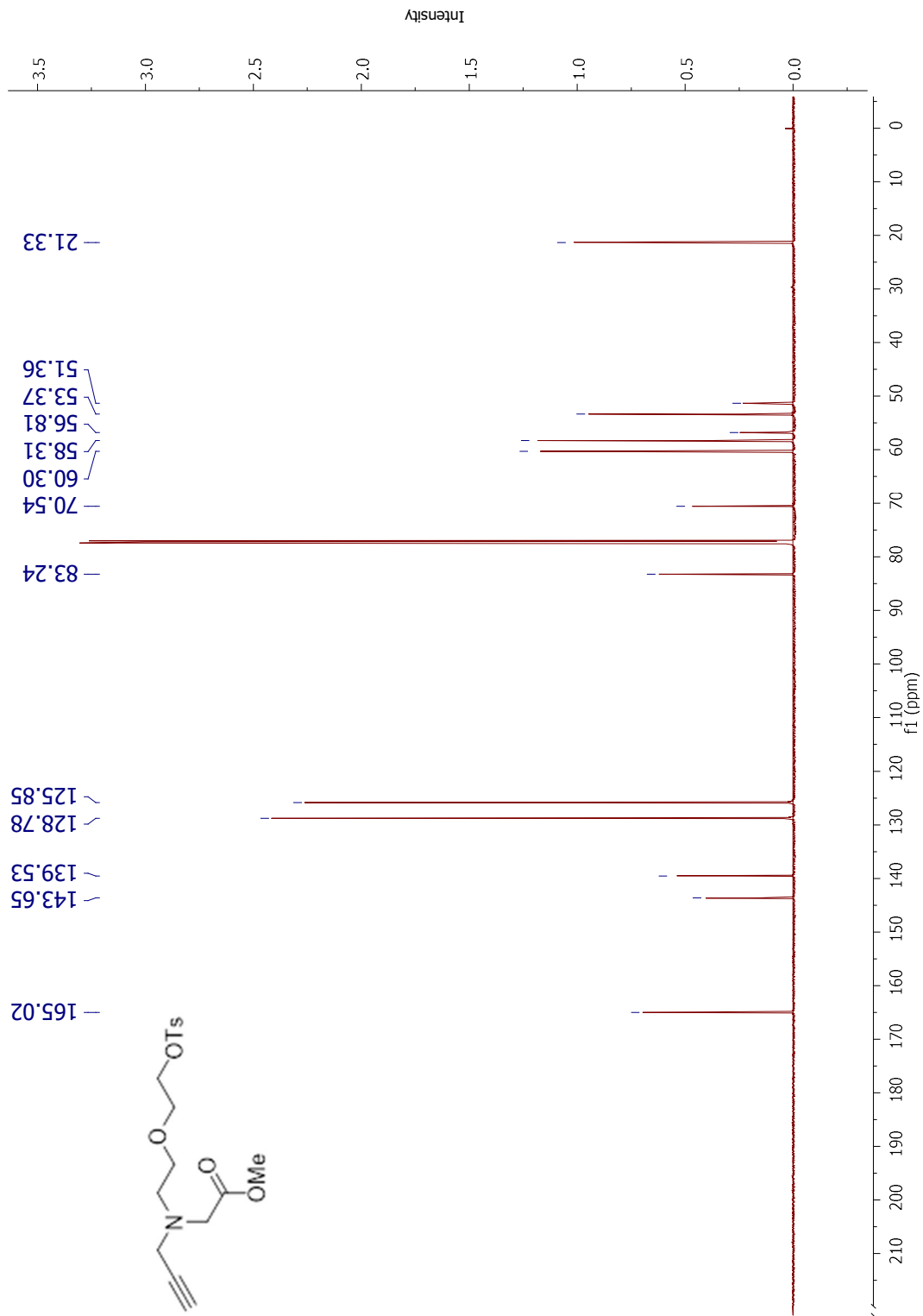


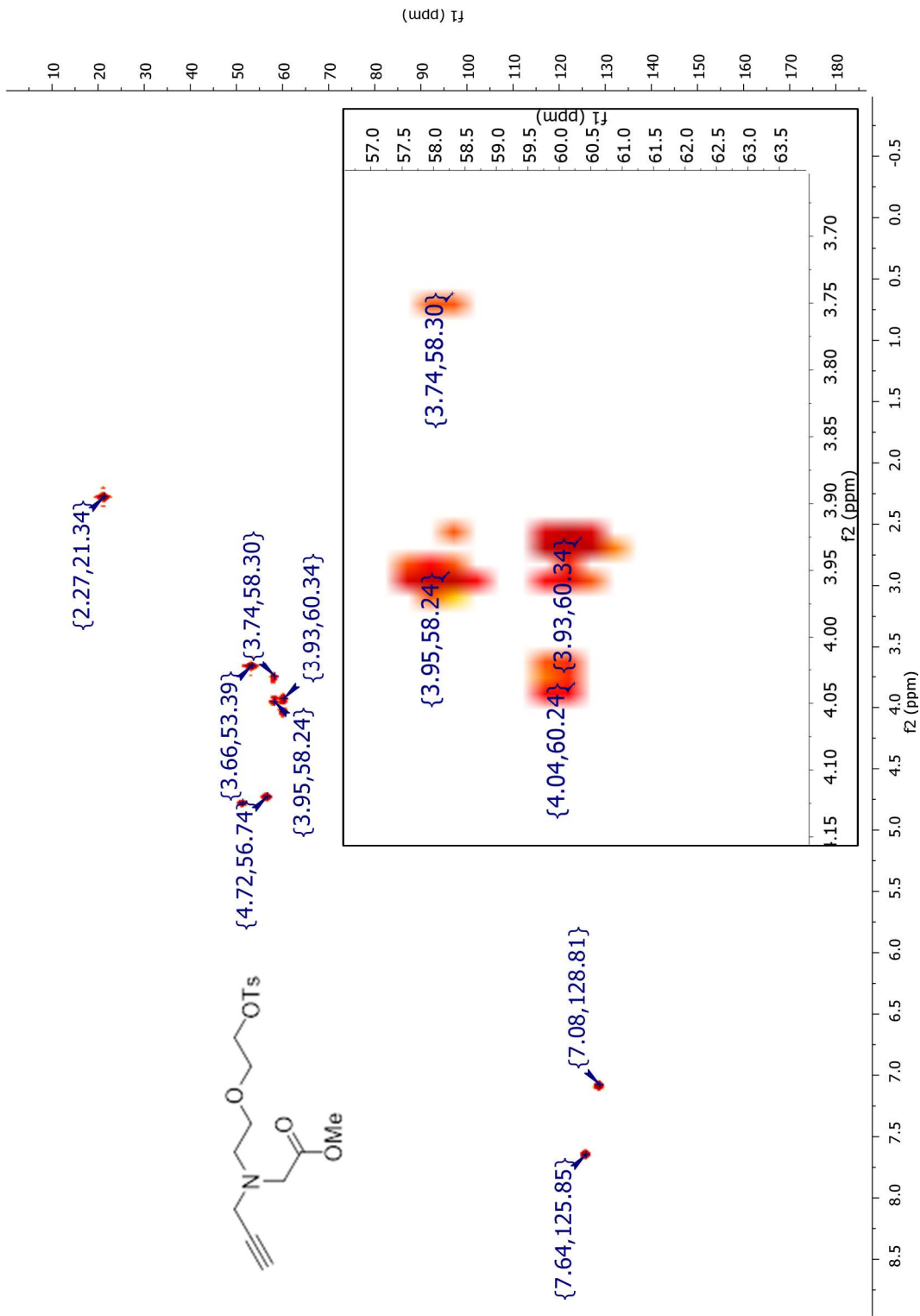
¹H NMR: Methyl 2-((2-(2-hydroxyethoxy)ethyl)(prop-2-ynyl)amino)acetate (3.5)





¹H NMR: Methyl 2-(prop-2-ynyl(2-(2-(tosyloxy)ethoxy)ethyl)amino)acetate (3.15)





HMQC: Methyl 2-(prop-2-ynyl(2-(2-(tosyloxy)ethoxy)ethyl)amino)acetate (3.15)